Representation of High-Dimensional Solid-Liquid Phase Diagrams of Ionic Systems

Ketan D. Samant and Ka M. Ng
Dept. of Chemical Engineering, University of Massachusetts, Amherst, MA 01003

A generic framework is presented for representation of the solid-liquid phase behavior of multicomponent ionic systems with and without compound formation. Isothermal isobaric phase behavior is represented in form of digraphs. The invariant points in the composition space are identified as vertices of the digraph. These vertices are connected by edges identified from the adjacency matrix, which is constructed by using a set of generic rules based on Gibbs phase rule. These edges form the boundaries of high-dimensional saturation varieties, which are identified from the saturation variety matrix. For graphical representation, the number of independent coordinates is calculated and a suitable set of coordinates is developed. Projections are used to view high-dimensional phase diagrams in their entirety and to simplify the analysis of the phase behavior. Potential applications of this framework include facilitation of experimental development and computer-aided design of crystallization-based separation processes.

Introduction

Ionic systems are encountered in a number of industrially important processes. Crystallization-based separations, wastewater treatment, seawater desalination, hydrometallurgical processes, and phase-transfer catalysis are a few examples. More specifically, a wide variety of inorganic salts are separated by crystallization-based techniques. For example, minerals such as borax, potash, sodium carbonate, and sodium chloride are crystallized from brines (Mehta, 1988; Jongema, 1993; Efraim et al., 1996). Sodium tripolyphosphate is precipitated from solutions of soda ash and orthophosphoric acid (Ainsworth, 1994). Of equal importance is the crystallization of organic salts to resolve optically active fine chemicals and pharmaceuticals (Paul and Rosas, 1990; Meul, 1992; Stinson, 1994; Schroer et al., 2001).

Clearly, the solid-liquid phase equilibria of ionic systems are of great importance for research and development in the chemical industry. For this reason, over the years, many authors have treated this subject in detail. The focus has been on experimental and theoretical development of thermodynamically consistent models and correlations (Meissner and Tester, 1972; Pitzer, 1973, 1975; Meissner and Kusik, 1973, 1979; Fuyuhiro et al., 1979; Sander et al., 1986; Nicolaisen et al., 1993; among others), and computer-aided simulation (Liu and Watanasari, 1999; Rafal et al., 2000). During the synthesis stage of process development, the design engineer has to generate and evaluate alternative process flowsheets. Synthesis of process flowsheets relies heavily on the insights obtained from visualization and analysis of the phase behavior of the system under consideration (Berry and Ng, 1996; Cisternas, 1999; Wibowo and Ng, 2000). Therefore, representation of the phase behavior of ionic systems, especially that of high-dimensional multicomponent systems, is an area of great importance from process synthesis point of view. However, this area has received little attention.

The objective of this article is to fill in this void with a systematic framework. It builds on the idea of representing high-dimensional solid-liquid phase diagrams in the form of directed graphs (digraphs) and associated matrices. In the following section, we summarize the basic concepts behind the framework. Then, we discuss the extensions to high-dimensional ionic systems. The issues addressed are thermodynamics, graphical representation, generation of digraphs, and identification of saturation varieties. These ideas are illus-

Correspondence concerning this article should be addressed to K. M. Ng at the following current address: Dept. of Chemical Engineering, Hong Kong University of Science and Technology, Clear Water Bay, Hong Kong.
Current address of K. D. Samant: Aspen Technology, Inc., Ten Canal Park, Cambridge, MA 02141-2201.

trated with three examples. The first two examples deal with ideal simple ionic systems. The third example considers a system with compound formation. Finally, we demonstrate the use of the framework for synthesizing crystallization process flowsheets with an industrial process.

Summary of Adjacency Rules

The central idea is to represent the phase behavior in the form of directed graphs (digraphs). This idea was used earlier by Samant et al. (2000) for high-dimensional molecular solid-liquid phase diagrams. Following is a summary of the definitions and rules related to this representation.

A *graph, $G = (V, E)$,* is a discrete mathematical model consisting of a set of vertices V and a set of edges E joining these vertices. A *digraph* is a graph in which each edge $e_{ij} = (v_i, v_j)$ has a direction from its "initial point" i to its "terminal point" j. The main advantage of representing the phase behavior in the form of digraphs is that the digraphs can be represented in the form of matrices. This is particularly useful for computer-aided generation and visualization of phase diagrams for process synthesis. The most useful is the adjacency matrix defined as follows (Biggs, 1993).

Definition: (Adjacency Matrix, $A = (a_{ij})$, of a digraph G)

$$a_{ij} = \begin{cases} 1 & \text{if } G \text{ has a directed edge } e_{ij} = (v_i, v_j) \\ 0 & \text{else} \end{cases} \tag{1}$$

The row and column headings of the adjacency matrix correspond to the vertices of the digraph. This matrix contains information on how these vertices are connected, or in other words it indicates the edges of the digraph. It is constructed by using the following set of rules:

Rule 1. *v_i is adjacent to v_j ($a_{ij} = 1$) if:*

- *v_j has more components than v_i and has all the components in v_i.*
- *All components saturated at v_i are also saturated at v_j.*
- *v_j has one additional saturated component.*

Rule 2. *v_i is adjacent to v_i ($a_{ij} = 1$) if:*

- *v_i and v_j have the same number of saturated components.*
- *All the components saturated at v_i are also saturated at v_j.*

Rule 3. *v_i is adjacent to v_j ($a_{ij} = 1$) if:*

- *v_i and v_j have the same components and the same number of saturated components.*
- *All but one component saturated at v_i are also saturated at v_j.*

These adjacency rules were derived earlier and the interested reader is referred to Samant et al. (2000).

Representation of Phase Diagrams

Solid-liquid phase equilibrium in ionic systems

Let us consider a system with m cations ($M_1, M_2, \ldots, M_m$) with positive charges of magnitudes ($z_{M_1}, z_{M_2}, \ldots, z_{Mm}$), n anions ($N_1, N_2, \ldots, N_n$) with negative charges of magnitudes ($z_{N_1}, z_{N_2}, \ldots, z_{N_n}$), and one solvent I. The criterion for solid-liquid equilibrium is that the chemical potential of the salt be equal to the sum of the chemical potentials of its constituents. Therefore, for example, in a solution saturated with salt $S = v_M M_i v_N N_j$ (here, $\frac{v_M}{v_N} = \frac{z_{N_j}}{z_{M_i}}$)

$$\frac{\mu_{M_i}}{v_N} + \frac{\mu_{N_j}}{v_M} = \frac{\mu_S}{v_M v_N} \tag{2}$$

The chemical potential of the ions is defined as (for example for M_i)

$$\mu_{M_i} = \mu^*_{M_i} + RT \ln\left(\gamma^*_{M_i}[M_i]\right) \tag{3}$$

The asterisk superscript indicates that infinite dilution standard state (asymmetric normalization) is used. The asymmetric molal activity coefficients are defined as (Pitzer, 1995)

$$\gamma^*_{M_i} = \frac{\hat{f}_{M_i}}{\hat{f}^*_{M_i}([M_i]/[M_i^o])}, \tag{4}$$

where the fugacity at the standard state is given by

$$\hat{f}^*_{M_i} = \lim_{[M_i]\to 0} \frac{\hat{f}_{M_i}}{[M_i]/[M_i^o]}, \qquad [M_{j\neq i}] = 0 \tag{5}$$

$[M_i^o] = 1\ \text{mol}-\text{kg}^{-1}$ and is used to cancel the dimensionality of $[M_i]$. The salt is in solid phase. Therefore, $\mu_S = \mu^o_S$. Using these definitions in Eq. 4, we can write for a solution saturated with salt S

$$\left(\gamma^*_{M_i}[M_i]\right)^{1/v_N}\left(\gamma^*_{N_j}[N_j]\right)^{1/v_M} = \exp\left[-\frac{1}{RT}\left(\frac{\mu^*_{M_i}}{v_N} + \frac{\mu^*_{N_j}}{v_M} - \frac{\mu^o_S}{v_M v_N}\right)\right]$$

$$K^I_S = K^{sp}_S(T) \tag{6}$$

The expression on the lefthand side K^I_S is the ionic product of salt S (product of ionic activities). The expression on the righthand side $K^{sp}_S(T)$ is the solubility product of salt S. The criterion for solid-liquid equilibrium is simply the equality of the ionic and solubility products at the specified temperature and pressure. When $K^I_S < K^{sp}_S$, the solution is unsaturated with salt S. Equilibrium criteria for other salts can also be obtained similarly. For example, let us consider the case of solvate formation. For a salt $\tilde{S} = v_M M_i v_N N_j \cdot kI$, at equilibrium

$$\frac{\mu_{M_i}}{v_N} + \frac{\mu_{N_j}}{v_M} + \frac{k\mu_I}{v_M v_N} = \frac{\mu_{\tilde{S}}}{v_M v_N} \tag{7}$$

For the solvent I, the chemical potential is defined as

$$\mu_I = \mu^o_I + RT\ln(\gamma_I x_I) \tag{8}$$

Superscript o indicates that the pure solvent standard state (symmetric normalization) is used. With this additional defi-

nition, the solubility product expression takes the following form

$$\left(\gamma^*_{M_i}[M_i]\right)^{1/\upsilon_N}\left(\gamma^*_{N_j}[N_j]\right)^{1/\upsilon_M}(\gamma_I x_I)^{k/\upsilon_M\upsilon_N} = \exp\left[-\frac{1}{RT}\left(\frac{\mu^*_{M_i}}{\upsilon_N}+\frac{\mu^*_{N_j}}{\upsilon_M}+\frac{k\mu^o_I}{\upsilon_M\upsilon_N}-\frac{\mu^o_S}{\upsilon_M\upsilon_N}\right)\right]$$

$$K^I_S = K^{sp}_S(T) \tag{9}$$

Note that the above expressions are on a one-equivalent basis in order to avoid raising the activity coefficients and molalities to high powers. To calculate the solid-liquid phase behavior of an ionic system by using these equations, we need data on the solubility products and a thermodynamic model for activity coefficients. Adequate data on solubility products of many salts can be obtained from sources such as Linke and Seidell (1965), Silcock (1979), and Zemaitis et al. (1986). A thermodynamic model and associated parameters may not be available for many systems. In such cases ideality (or any suitable approximation) may be assumed as a starting point.

Graphical representation

In this subsection, let us discuss the various means of graphical representation of the phase behavior of high-dimensional ionic systems. We are primarily interested in the isothermal isobaric phase behavior of systems with two or more cations and anions and one solvent.

Let us revisit the system of m cations, n anions, and one solvent I. Consider first the case of a simple ionic system in which no compounds (solvates or multiple salts) are formed. The m cations and n anions can form a total of mn simple salts. Therefore, we have a total of $c = mn+1$ components. Let us now construct the invariance matrix B for the system (Waller and Mäkilä, 1981). The column headings of this matrix are the components (mn salts and 1 solvent) and the row headings are the reaction invariants (in this case $m+n$ ions and 1 solvent). The matrix entries are the stoichiometric coefficients. For example, for a simple ionic system A^+, B^+, X^-, Y^-, I (salts AX, AY, BX, and BY), the invariance matrix B is

	AX	AY	BX	BY	I
A^+	1	1	0	0	0
B^+	0	0	1	1	0
X^-	1	0	1	0	0
Y^-	0	1	0	1	0
I	0	0	0	0	1

(10)

It can be shown (see Appendix A) that for any system, rank(B) = $m+n$. Therefore, we can have $r = c - \text{rank}(B) = (m-1)(n-1)$ independent reactions describing the system. For the above system, we have the following independent reaction [$r = (2-1)(2-1) = 1$]

$$AX + BY \Leftrightarrow AY + BX \tag{11}$$

At thermodynamic equilibrium, the presence of r independent reactions reduces the dimensionality of the phase diagram by r. Therefore, instead of $c-1$ mole fraction coordinates, we will need $c-r-1$ independent coordinates to represent the phase behavior graphically.

Now let us consider the case of compound formation. The compounds are formed between two or more salts and/or the solvent. Each compound formed increases the number of components by one. Also, the formation of each compound can be written as one independent reaction. Therefore, the number of independent reactions also increases by one, thereby conserving the dimensionality of the system and the number of independent coordinates.

Before proceeding further, a brief discussion on the independent coordinates is in order. The nature of these coordinates will depend on the reaction invariants we choose as the row entries to the invariance matrix. For example, a certain choice of invariants will lead to the transformed mole fraction coordinates of Ung and Doherty (1995a). Another choice will lead to the element mole fractions of Pérez Cisneros et al. (1997). The choice of the invariants is dictated by the suitability to the application or some constraints imposed by the equilibrium equations. For example, the transformed mole fraction coordinates are suitable for describing the equilibrium phase behavior of molecular reactive systems (Ung and Doherty, 1995b; Berry and Ng, 1997; Samant and Ng, 1998), and the element mole fractions are useful for reactive flash calculations. Whatever the choice of the invariants, the resulting independent coordinates share the following properties:

- They are independent of the extents of reactions.
- One set of coordinates is an algebraic function of another set of coordinates (the functionality depends on the system under consideration). For example, for a given system, the element mole fractions of Pérez Cisneros et al. can be expressed as algebraic functions of the transformed mole fractions of Ung and Doherty.

Now let us move on to the problem of selecting the independent coordinates for ionic systems. Here, as seen in the previous subsection, the thermodynamic information is available in terms of solubility products which are equated to the ionic products (products of molal ionic activities). Therefore, it is natural and extremely convenient to express the independent coordinates as functions of molal ionic concentrations. Note that this is the reason we chose the ions and the solvent as the invariants (row headings of the invariance matrix). The following choices may be made for the $c-r-1 = m+n-1$ independent coordinates.

- $m-1$ coordinates related to the cation compositions

$$R(M_i) = \frac{z_{M_i}[M_i]}{\sum_{j=1}^{m} z_{M_j}[M_j]} \qquad i = 1, \ldots, m-1, \tag{12}$$

- $n-1$ coordinates related to the anion compositions

$$R(N_i) = \frac{z_{N_i}[N_i]}{\sum_{j=1}^{n} z_{N_j}[N_j]} \qquad i = 1, \ldots, n-1, \text{ and} \tag{13}$$

- 1 coordinate related to the solvent composition

$$\frac{1}{s} = \frac{1}{\sum_{j=1}^{m} z_{M_j}[M_j]} = \frac{1}{\sum_{j=1}^{n} z_{N_j}[N_j]}. \qquad (14)$$

$R(M_i)$ may be interpreted as the cationic equivalent fraction of M_i, $R(N_i)$ as the anionic equivalent fraction of N_i, and $1/s$ as the mass of solvent per equivalent of the salts. Note that this is by no means the only set of independent coordinates that can be used. Many other sets could be constructed. However, this choice is preferred as it preserves the linearity of material balance equations (see Appendix B). An interesting aspect to note is that for this coordinate scheme, the solvent coordinate $1/s$ is not bounded.

As discussed above, the isothermal isobaric phase diagram has $c - r - 1 = m + n - 1$ dimensions. For $m + n \geq 4$ (which is always the case as $m \geq 2$ and $n \geq 2$), these phase diagrams cannot be plotted in two dimensions in their original form. In order to plot them in two dimensions, we need to reduce the dimensionality through proper use of projections. The different ways in which this can be done are shown in Figure 1.

For $m + n \geq 4$, to make the graphical representation more useful, the solvent coordinate ($1/s$) is eliminated first. This can be accomplished by an *orthogonal projection* of the original phase diagram. Elimination of the solvent coordinate reduces the dimensionality by one to $m + n - 2$. Therefore, this projection can be plotted in two dimensions only for systems with $m + n = 4$ ($m = 2$, $n = 2$). For $m + n \geq 5$, it is still not possible to plot the phase diagram in two dimensions. In this situation, we can plot the phase diagram as a set of projections; each projection is plotted by neglecting the molal compositions of all but two cations and two anions. We can plot a total of $\binom{m}{2}\binom{n}{2}$ projections. As we will see later with the aid of examples, on any one of these projections, the saturation varieties corresponding to the salts formed entirely by the ignored ions cannot be seen. However, the information regarding these saturation varieties is not lost as they appear on other projections.

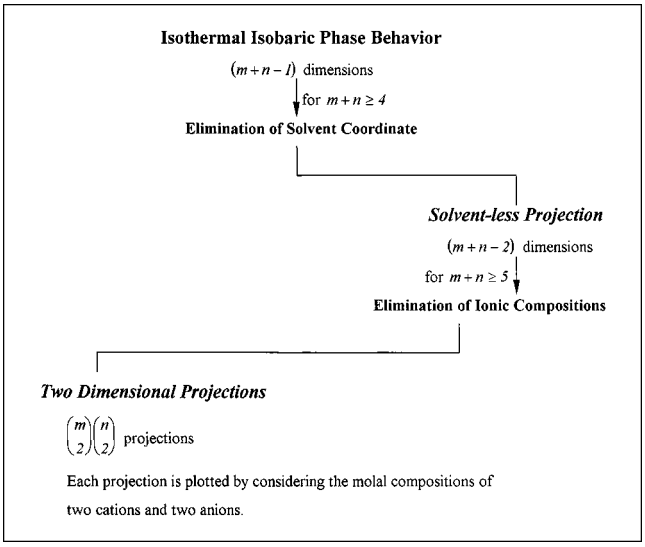

Figure 1. Graphical representation of phase diagrams.

Constructing the digraphs

The systematic procedure for constructing the digraphs is described below. We denote the isothermal isobaric phase diagram of a multicomponent ionic system by a digraph $G_{PT}^{I} = (V_{PT}^{I}, E_{PT}^{I})$. Subscripts P and T indicate constant pressure and temperature, respectively. The superscript I refers to ionic systems.

Identification and Location of the Vertices: Simple Ionic Systems. Let us return to the system of m cations, n anions, and one solvent. According to Gibbs phase rule, at a specified temperature and pressure, the maximum number of salts that can precipitate together is $p = c - r - 1 = m + n - 1$. The saturation varieties where $m + n - 1$ salts are saturated will occur as vertices [$f = c - (p + 1) - r = 0$]. These vertices can easily be identified by applying the following screening criteria to all $\binom{mn}{m+n-1}$ combinations of $m + n - 1$ salts out of the possible mn:

Criterion 1. All ions under consideration must be present in the system.

Criterion 2. Any pair of saturated salts must either have a common ion or must be compatible.

The compatibility test for a salt pair is given in Appendix C.

There are additional vertices that correspond to saturation varieties where lesser number of salts are saturated. However, as $f = 0$ at any vertex, these vertices have lesser number of ions. For example, vertices where $m + n - 2$ salts are saturated must contain one less ion than the vertices where $m + n - 1$ salts are saturated and vertices where $m + n - 3$ salts are saturated must contain two less ions than the vertices where $m + n - 1$ salts are saturated. To identify vertices with $m + n - 2$ saturated salts, we delete each cation and each anion in turn and again screen all $m\binom{(m-1)n}{m+n-2} + n\binom{m(n-1)}{m+n-2}$ combinations using the above criteria. This procedure is repeated to identify vertices with still lesser number of saturated salts by deleting the requisite number of ions. Note that while removing the requisite number of ions from the system, care must be taken to keep at least one cation and one anion in the system.

The location of a vertex refers to the value of the independent coordinates associated with the vertex. These locations are determined by using the solubility product information at the specified temperature. The algorithm for locating the vertices is given in Table 1. If a thermodynamically consistent model is not available for predicting the activity coefficients, ideality may be assumed.

Identification and Location of the Vertices: Systems with Compound Formation. For systems with compound formation, solvates and multiple salt compounds can exist. However, as each additional compound is a result of an additional reaction, the maximum number of salts that can precipitate remains the same and equal to $m + n - 1$. Vertices where $m + n - 1$ salts are saturated must contain all the ions in the system. Along similar lines, vertices where $m + n - 2$ salts are saturated must contain one less ion than the vertices where $m + n - 1$ salts are saturated, and so on. In this case, however, no simple screening criteria can be used for identification of the vertices. The tasks of identification and location are performed simultaneously by using the screening algorithm given in Table 2. To use this algorithm, all the com-

Table 1. Algorithm for Location of Vertices $\in V_{PT}^I$ for Simple Ionic Systems

• Consider a system of m cations (M_1, M_2, …, M_m), n anions (N_1, N_2, …, N_n), and one solvent. • Consider a vertex $\in V_{PT}^I$, at which the system has p ($1 \le p \le m$) cations (M_1, M_2, …, M_p), q ($1 \le q \le n$) anions (N_1, N_2, …, N_q), and the solvent. ($[M_{p+1}] = \cdots = [M_m] = [N_{q+1}] = \cdots = [N_n] = 0$). • At this vertex, we have $p+q-1$ saturated salts, $p+q$ variables ($[M_i]$, $i=1, 2, \ldots, p$, and $[N_i]$, $i=1, 2, \ldots, q$), and $p+q$ equations: — $p+q-1$ phase equilibrium equations $K_i^{sp} = K_i^I$, $i=1, 2, \ldots, p+q-1$, for the saturated salts, —One equation for electroneutrality of the system $\sum_{i=1}^{p} z_{M_i}[M_i] = \sum_{i=1}^{q} z_{N_i}[N_i]$.
(1) Initialize $\gamma_{M_i}^*$, $i=1, 2, \ldots, p$ and $\gamma_{N_i}^*$, $i=1, 2, \ldots, q$ to unity.
(2) Pick initial guesses for $[M_i]$, $i=1, 2, \ldots, p$ and $[N_i]$, $i=1, 2, \ldots, q-1$. Calculate $[N_q]$ from the condition of electroneutrality.
(3) Calculate $\gamma_{M_i}^*$, $i=1, 2, \ldots, p$ and $\gamma_{N_i}^*$, $i=1, 2, \ldots, q$ using a thermodynamically consistent model.
(4) Calculate the following $p+q-1$ functions: $F(i) = K_i^I - K_i^{sp}$ (index i denotes a saturated salt).
(5) If $\lvert F \rvert > \boldsymbol{\epsilon}$ (a vector of set tolerances) then go to step 2 and simultaneously update the values of the guesses. For updating the guesses, use Newton's method with a finite difference approximation to the Jacobian. Otherwise, go to step 6.
(6) Calculate the independent coordinates $R(M_j)$ ($j=1, 2, \ldots, m-1$), $R(N_j)$ ($j=1, 2, \ldots, n-1$), and $1/s$.

pounds that can possibly form in the pressure and temperature range of interest must be known. The equations to be solved are the same as the algorithm of Table 1. The difference lies in steps 1 and 7, which perform the task of screening (identification); while steps 2 to 6 perform the task of locating the vertices as before. The use of the screening algorithm for all $m+n$ ions gives the vertices with $m+n-1$ saturated salts, for all combinations with $m+n-1$ ions gives the vertices with $m+n-2$ saturated salts, and so on.

Table 2. Algorithm for Screening of Vertices $\in V_{PT}^I$ for Systems with Compound Formation

• The system, the variables, and the equations are the same as the algorithm of Table 1. • In this algorithm, identification and location of vertices is done simultaneously. Steps 2 to 6 locate the vertices as was done in the algorithm of Table 1. The additional steps, step 1 and step 7, perform the task of identification.
1) Consider all combination of $p+q-1$ salts that can be saturated. For each combination follow steps 2 to 7.
(2) Initialize $\gamma_{M_i}^*$, $i=1, 2, \ldots, p$ and $\gamma_{N_i}^*$, $i=1, 2, \ldots, q$ to unity.
(3) Pick initial guesses for $[M_i]$, $i=1, 2, \ldots, p$ and $[N_i]$, $i=1, 2, \ldots, q-1$. Calculate $[N_q]$ from the condition of electroneutrality.
(4) Calculate $\gamma_{M_i}^*$, $i=1, 2, \ldots, p$ and $\gamma_{N_i}^*$, $i=1, 2, \ldots, q$ using a thermodynamically consistent model.
(5) Calculate the following $p+q-1$ functions: $F(i) = K_i^I - K_i^{sp}$ (index i denotes a saturated salt).
(6) If $\lvert F \rvert > \boldsymbol{\epsilon}$ (a vector of set tolerances) then go to step 3 and simultaneously update the values of the guesses. For updating the guesses, use Newton's method with a finite difference approximation to the Jacobian. Otherwise go to step 7.
(7) If the solution is consistent, accept the vertex and calculate the independent coordinates $R(M_j)$ ($j=1, 2, \ldots, m-1$), $R(N_j)$ ($j=1, 2, \ldots, n-1$), and $1/s$. A consistent solution is one for which the following conditions are satisfied in addition to the condition of step 6: • $[M_j]$ and $[N_j]$ are positive $\forall j$. • $K_j^I < K_j^{sp}$, $\forall j$ where index j denotes an unsaturated salt.

Table 3. Algorithm for Calculation of Edges $\in E_{PT}^I$ using a Thermodynamic Model

• Consider an edge $e_{ij} = (v_i, v_j) \in E_{PT}^I$ along which we have p cations (M_1, M_2, …, M_p), q anions (N_1, N_2, …, N_q), and the solvent. • Along this edge, we have $p+q-2$ saturated salts, $p+q$ variables, and $p+q-1$ equations (similar to the equations of Tables 1 and 2). • This edge will have at least one vertex (v_i) at which an additional salt is saturated. We will start the calculation from this vertex.
(1) Initialize $\gamma_{M_i}^*$, $i=1, 2, \ldots, p$ and $\gamma_{N_i}^*$, $i=1, 2, \ldots, q$ to unity.
(2) Let the saturated salts be denoted by indices 1 to $p+q-2$ and the additional saturated salt in the vertex by index $p+q-1$.
(3) Vary the molal composition of a suitable ion (denoted as M_p) starting from $[M_p]_{v_i}$. Follow the following steps for each value of M_p. Stop when the other vertex v_j is reached.
(4) Pick initial guesses for $[M_i]$, $i=1, 2, \ldots, p-1$ and $[N_i]$, $i=1, 2, \ldots, q-1$. At $[M_p] = [M_p]_{v_i}$, use $[M_i] = [M_i]_{v_i}$, $i=1, 2, \ldots, p-1$ and $[N_i] = [N_i]_{v_i}$, $i=1, 2, \ldots, q-1$ as initial guesses. For other values of $[M_p]$, use the values from the previous calculation. Calculate $[N_q]$ from the condition of electroneutrality.
(5) Calculate $\gamma_{M_i}^*$, $i=1, 2, \ldots, p$ and $\gamma_{N_i}^*$, $i=1, 2, \ldots, q$ using a thermodynamically consistent model.
(6) Calculate the following $p+q-2$ functions: $F(i) = K_i^I - K_i^{sp}$, $i=1, 2, \ldots, p+q-2$.
(7) If $\lvert F \rvert > \boldsymbol{\epsilon}$ (a vector of set tolerances), then go to step 4 and simultaneously update the values of the guesses. For updating the guesses, use Newton's method with a finite difference approximation to the Jacobian. Otherwise go to Step 8.
(8) For each solution, calculate the independent coordinates $R(M_i)$ ($i=1, 2, \ldots, m-1$), $R(N_i)$ ($i=1, 2, \ldots, n-1$), and $1/s$.

For all systems (with or without compound formation), the vertices are labeled after the salts that are saturated. The unsaturated salts and the solvent are written as subscripts.

Identification and Calculation of the Edges. Once all the vertices are identified and located, the adjacency matrix can be constructed by using the adjacency rules discussed before. The edges can be identified by reading across the rows of the adjacency matrix. For accurate graphical representation of the phase behavior, it is essential that the edges thus identified are calculated as accurately as possible. The algorithm for calculation of the edges is given in Table 3. Again, in the absence of a thermodynamic model for activity coefficients, ideality may be assumed.

Identification of saturation varieties

The edges of the digraph form the boundaries of various saturation varieties. For conceptual design of crystallization-based separation processes, it is sufficient to just identify these

saturation varieties. For more quantitative design methods, we need to express them in the form of algebraic equations (Pressly and Ng, 1999). However, it is not apparent from the adjacency matrix, which saturation varieties are bounded by which edges. For this purpose, the saturation variety matrix is more useful. The row headings of this matrix correspond to the saturation varieties and the column headings correspond to the vertices of the corresponding digraph. This matrix can be formally defined as follows:

Definition. (Saturation Variety Matrix, $S = (s_{ij})$)

$$s_{ij} = \begin{cases} 1 & \text{if vertex } v_j \text{ lies on the saturation variety} \\ & \text{represented by row } i \\ 0 & \text{else} \end{cases} \quad (15)$$

For a given digraph, the saturation varieties that are present are obtained from the components saturated at the vertices and along the edges. For example, as we will see later, vertex AX_I implies the presence AX-saturation variety and edge $AX\ AY\ BX_{BYI} - AY\ BX\ BY_{AXI}$ implies the presence of $AY\ BX -$ double saturation variety. To construct S, first the vertices are listed as column headings and all the saturation varieties are listed as row headings. The matrix is then constructed as

$$s_{ij} = \begin{cases} 1 & \text{if all components saturated in the row heading} \\ & \text{are also saturated in the column heading} \\ 0 & \text{else} \end{cases} \quad (16)$$

Once the saturation variety matrix is constructed, the saturation varieties on the phase diagrams can easily be identified by reading across its rows. When the composition of a process stream is known, we can identify the components that are saturated in this stream from the saturation variety this stream lies within.

With these tools, the framework for representation of high-dimensional phase diagrams of multicomponent ionic systems is complete. We are now in a position to visualize these phase diagrams for process synthesis. Let us consider a few examples to illustrate the framework. Before proceeding, we would like to point out that thus far, we have focused our attention on solutions of strong electrolytes. The framework, however, is also applicable to more complex ionic systems as discussed in Appendix D.

Examples

Example 1: quaternary conjugate salt system

To set the stage, let us begin with a simple example of a quaternary conjugate salt system. The system comprises cations A^+, B^+ ($m = 2$), anions X^-, Y^- ($n = 2$), and solvent I. The ions can form four simple salts, viz., AX, AY, BX, and BY. We will refer to these salts as $S1$, $S2$, $S3$, and $S4$, respectively, for the sake of convenience. The system is assumed to behave ideally. The solubility products for the four salts at 298.15 K and 1 atm are listed in Table 4. Let us first construct the digraph for the isothermal isobaric phase behavior.

Table 4. Solubility Products for Example 1 at 298.15 K and 1 atm

Salt	Ionic Product	Solubility Product
AX ($S1$)	$[A^+][X^-]$	0.4
AY ($S2$)	$[A^+][Y^-]$	0.2
BX ($S3$)	$[B^+][X^-]$	0.1
BY ($S4$)	$[B^+][Y^-]$	0.3

At 298.15 K and 1 atm, the solubility products are such that $K^{sp}_{S2}K^{sp}_{S3} < K^{sp}_{S1}K^{sp}_{S4}$. Therefore, salts $S2$ and $S3$ form the compatible salt pair and salts $S1$ and $S4$ are incompatible. The maximum number of salts that can precipitate from this system is $m + n - 1 = 3$. The vertices where three salts are saturated must contain all four ions in solution. As salts $S2$ and $S3$ are compatible, we have two such vertices, $S1S2S3_{S4I}$ and $S2S3S4_{S1I}$. Vertices with two saturated salts will have only three ions in solution. We can form four systems with three ions in solution by deleting one ion in turn. Each of these systems gives one vertex at which two salts are saturated. These vertices are $S1S2_I$, $S1S3_I$, $S2S4_I$, and $S3S4_I$. Vertices with one saturated salt will have only two ions in solution (one cation and one anion). Therefore, these vertices are $S1_I$, $S2_I$, $S3_I$, and $S4_I$. The locations of these vertices are listed in Table 5. Note that for this system, the algorithm of Table 1 can be used to express the locations of vertices in the form of simple algebraic functions of the solubil-

Table 5. Locations of the Vertices for Example 1 at 298.15 K and 1 atm

Vertex	Location $R(A^+)$	Location $R(X^-)$	1/s
One Saturated Salt			
$S1_I$	1	1	$\frac{1}{\sqrt{K^{sp}_{S1}}}$
$S2_I$	1	0	$\frac{1}{\sqrt{K^{sp}_{S2}}}$
$S3_I$	0	1	$\frac{1}{\sqrt{K^{sp}_{S3}}}$
$S4_I$	0	0	$\frac{1}{\sqrt{K^{sp}_{S4}}}$
Two Saturated Salts			
$S1S2_I$	1	$\frac{K^{sp}_{S1}}{K^{sp}_{S1}+K^{sp}_{S2}}$	$\frac{1}{\sqrt{K^{sp}_{S1}+K^{sp}_{S2}}}$
$S1S3_I$	$\frac{K^{sp}_{S1}}{K^{sp}_{S1}+K^{sp}_{S3}}$	1	$\frac{1}{\sqrt{K^{sp}_{S1}+K^{sp}_{S3}}}$
$S2S4_I$	$\frac{K^{sp}_{S2}}{K^{sp}_{S2}+K^{sp}_{S4}}$	0	$\frac{1}{\sqrt{K^{sp}_{S2}+K^{sp}_{S4}}}$
$S3S4_I$	0	$\frac{K^{sp}_{S3}}{K^{sp}_{S3}+K^{sp}_{S4}}$	$\frac{1}{\sqrt{K^{sp}_{S3}+K^{sp}_{S4}}}$
Three Saturated Salts			
$S1S2S3_{S4I}$	$\frac{K^{sp}_{S1}}{K^{sp}_{S1}+K^{sp}_{S3}}$	$\frac{K^{sp}_{S1}}{K^{sp}_{S1}+K^{sp}_{S2}}$	$\sqrt{\frac{R(A^+)R(X^-)}{K^{sp}_{S1}}}$
$S2S3S4_{S1I}$	$\frac{K^{sp}_{S2}}{K^{sp}_{S2}+K^{sp}_{S4}}$	$\frac{K^{sp}_{S3}}{K^{sp}_{S3}+K^{sp}_{S4}}$	$\sqrt{\frac{R(A^+)[1-R(X^-)]}{K^{sp}_{S1}}}$

Adjacency Matrix

	$S1_I$	$S2_I$	$S3_I$	$S4_I$	$S1S2_I$	$S1S3_I$	$S2S4_I$	$S3S4_I$	$S1S2S3_{S4I}$	$S2S3S4_{S1I}$
$S1_I$	0	0	0	0	1	1	0	0	0	0
$S2_I$	0	0	0	0	1	0	1	0	0	0
$S3_I$	0	0	0	0	0	1	0	1	0	0
$S4_I$	0	0	0	0	0	0	1	1	0	0
$S1S2_I$	0	0	0	0	0	0	0	0	1	0
$S1S3_I$	0	0	0	0	0	0	0	0	1	0
$S2S4_I$	0	0	0	0	0	0	0	0	0	1
$S3S4_I$	0	0	0	0	0	0	0	0	0	1
$S1S2S3_{S4I}$	0	0	0	0	0	0	0	0	0	1
$S2S3S4_{S1I}$	0	0	0	0	0	0	0	0	1	0

Figure 2. Adjacency matrix for Example 1.

ity products as the system is ideal and all the ions are monovalent.

The adjacency matrix for the system is shown in Figure 2. This matrix reveals a total of 13 edges. Note for example that vertex $S1S2_I$ is adjacent to vertex $S1S2S3_{S4I}$ according to rule 1 and vertex $S1S2S3_{S4I}$ is adjacent to vertex $S2S3S4_{S1I}$ (and vice versa) according to rule 3. Salts $S1$ and $S2$ are saturated on edge $S1S2_I - S1S2S3_{S4I}$ and salts $S2$ and $S3$ are saturated on edge $S1S2S3_{S4I} - S2S3S4_{S1I}$. These edges can also be calculated as simple algebraic functions of the solubility products.

Let us now turn to the graphical representation of the digraph and identification of saturation varieties. The three independent coordinates (these coordinates were also used for the locations in Table 5) are

$$R(A^+) = \frac{[A^+]}{[A^+]+[B^+]}, \tag{17a}$$

$$R(X^-) = \frac{[X^-]}{[X^-]+[Y^-]}, \tag{17b}$$

and

$$\frac{1}{s} = \frac{1}{[A^+]+[B^+]}. \tag{17c}$$

The isothermal isobaric-phase diagram is three-dimensional (3-D). As shown in Figure 1, the solvent coordinate is eliminated to reduce the dimensionality by one. The solvent-less projection of the phase diagram has two dimensions and can be plotted easily as shown in Figure 3, which also shows the saturation variety matrix. The saturation varieties are identified from the projection and the saturation variety matrix. For example, the $S1$ saturation variety can be identified as the area enclosed by the edges connecting $S1_I$, $S1S2_I$, $S1S2S3_{S4I}$ and $S1S3_I$ and the $S2S3$ double saturation variety corresponds to the edge $S1S2S3_{S4I} - S2S3S4_{S1I}$.

When the solvent is removed gradually from an unsaturated (solvent-rich) process stream, depending upon the initial composition, different salts will start to crystallize. The salt(s) that will precipitate first can be identified from the 2-D projections of the phase diagram and the corresponding saturation variety matrix. For example, let us consider two process streams $P1$ ($[A^+] = 0.4$, $[B^+] = 0.1$, $[X^-] = 0.1$, and $[Y^-] = 0.4$) and $P2$ ($[A^+] = 0.05$, $[B^+] = 0.45$, $[X^-] = 0.125$ and $[Y^-] = 0.375$). Both the streams are unsaturated at 298.15 K and 1 atm. The locations of these streams are plotted on the projection of Figure 3. Stream $P1$ lies on the $S2$ saturation variety and stream $P2$ lies on the $S3S4$ double saturation variety. Therefore, as the solvent is removed gradually from these streams, salt $S2$ will precipitate first from stream $P1$ and salts $S3$ and $S4$ will precipitate together from stream $P2$. It must be noted that when the number of 2-D projections is greater than one, we need to plot the stream composition on each projection in order to uniquely ascertain which saturation variety the stream composition lies on.

Example 2: six salt simple ionic system

Now let us consider a more complicated simple ionic system with cations A^+, B^{2+}, anions X^-, Y^{2-}, Z^{3-}, and sol-

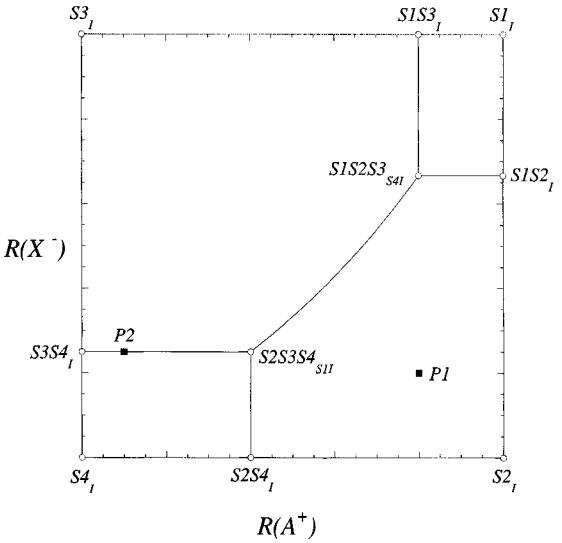

Saturation Variety Matrix

	$S1_I$	$S2_I$	$S3_I$	$S4_I$	$S1S2_I$	$S1S3_I$	$S2S4_I$	$S3S4_I$	$S1S2S3_{S4I}$	$S2S3S4_{S1I}$
$S1$–sat	1	0	0	0	1	1	0	0	1	0
$S2$–sat	0	1	0	0	1	0	1	0	1	1
$S3$–sat	0	0	1	0	0	1	0	1	1	1
$S4$–sat	0	0	0	1	0	0	1	1	0	1
$S1S2$–double sat	0	0	0	0	1	0	0	0	1	0
$S1S3$–double sat	0	0	0	0	0	1	0	0	1	0
$S2S4$–double sat	0	0	0	0	0	0	1	0	0	1
$S3S4$–double sat	0	0	0	0	0	0	0	1	0	1
$S2S3$–double sat	0	0	0	0	0	0	0	0	1	1

Figure 3. Solvent-less projection and saturation variety matrix for Example 1.

Table 6. Solubility Products for Example 2 at 298.15 K and 1 atm

Salt	Ionic Product	Solubility Product
AX ($S1$)	$[A^+][X^-]$	0.4
A_2Y ($S2$)	$[A^+][Y^{2-}]^{1/2}$	0.2
A_3Z ($S3$)	$[A^+][Z^{3-}]^{1/3}$	0.35
BX_2 ($S4$)	$[B^{2+}]^{1/2}[X^-]$	0.1
BY ($S5$)	$[B^{2+}]^{1/2}[Y^{2-}]^{1/2}$	0.3
B_3Z_2 ($S6$)	$[B^{2+}]^{1/2}[Z^{3-}]^{1/3}$	0.05

vent I. The ions can form six simple salts, viz., AX, A_2Y, A_3Z, BX_2, BY, and B_3Z_2. We will refer to these salts as $S1$, $S2$, $S3$, $S4$, $S5$, and $S6$, respectively. Let us consider the phase behavior of the system at 298.15 K and 1 atm. The solubility products for the six salts at this temperature and pressure are listed in Table 6.

The compatibility test reveals that salts ($S1$, $S6$), ($S2$, $S4$), and ($S2$, $S6$) form the compatible salt pairs. Using this information, the vertices are identified and listed in Table 7. We have a total of 26 vertices: 3 with four saturated salts, 8 with three saturated salts, 9 with two saturated salts, and 6 with one saturated salt. The locations of the vertices are calculated by assuming ideal behavior. In this case it is no longer possible to express the locations as simple algebraic functions of the solubility products.

The adjacency matrix (not shown for the sake of brevity) reveals a total of 49 edges. For example, as we will see later on the phase diagrams, vertex $S1S2_I$ is connected to vertex $S1S2S3_I$ according to rule 1. Salts $S1$ and $S2$ are saturated along this edge. Similarly, vertex $S1S2S3S6_{S4S5I}$ is connected to vertex $S1S2S4S6_{S3S5I}$ (and vice versa). Along this edge salts, $S1$, $S2$, and $S6$ are saturated. The edges are calculated using the algorithm of Table 3.

The four independent coordinates used for graphical representation of this system are

$$R(A^+) = \frac{[A^+]}{[A^+]+2[B^{2+}]}, \tag{18a}$$

$$R(X^-) = \frac{[X^-]}{[X^-]+2[Y^{2-}]+3[Z^{3-}]}, \tag{18b}$$

$$R(Y^{2-}) = \frac{2[Y^{2-}]}{[X^-]+2[Y^{2-}]+3[Z^{3-}]}, \quad \text{and} \tag{18c}$$

$$\frac{1}{s} = \frac{1}{[A^+]+2[B^{2+}]}. \tag{18d}$$

The isothermal isobaric phase behavior has 4 dimensions. The solvent-less projection obtained by elimination of the solvent coordinate decreases the dimensionality to 3. This projection can be plotted in form of a prism as shown in Figure 4. Each rectangular face of the prism represents a quaternary conjugate salt system comprising of cations A^+, B^{2+}, and anions X^-, Y^{2-}; X^-, Z^{3-}; or Y^{2-}, Z^{3-}. Each triangular face represents a system of three salts with a common cation (A^+ or B^{2+}). Note that these triangular faces are equivalent to the isothermal isobaric phase diagrams of molecular systems with three solutes (the three salts) and one solvent (Samant et al., 2000). The 6 vertices with one saturated salt form the vertices of the prism (for example $S1_I$ and $S4_I$). The 9 vertices with

Table 7. Vertices for Example 2 at 298.15 K and 1 atm

One Salt	Two Salts	Three Salts	Four Salts
$S1_I$	$S1S2_I$	$S1S2S3_I$	$S1S2S3S6_{S4S5I}$
$S2_I$	$S1S3_I$	$S1S2S4_{S5I}$	$S1S2S4S6_{S3S5I}$
$S3_I$	$S2S3_I$	$S1S3S6_{S4I}$	$S2S4S5S6_{S1S3I}$
$S4_I$	$S4S5_I$	$S1S4S6_{S3I}$	
$S5_I$	$S4S6_I$	$S2S3S6_{S5I}$	
$S6_I$	$S5S6_I$	$S2S4S5_{S1I}$	
	$S1S4_I$	$S2S5S6_{S3I}$	
	$S2S5_I$	$S4S5S6_I$	
	$S3S6_I$		

two saturated salts lie on the nine bounding edges of the prism (for example $S1S4_I$). The 8 vertices with three saturated salts lie on the faces of the prism; two each on the three rectangular faces (for example, $S1S4S6_{S3I}$) and one each on the two triangular faces (for example, $S1S2S3_I$). Finally, the 3 vertices with four saturated salts lie within the prism (for example, $S1S2S4S6_{S3S5I}$) and are shown as filled squares. To simplify the representation of the phase diagram, we need to plot it in form of 2-D projections. We need three figures to completely represent the above solvent-less projection in two dimensions. These 2-D projections are shown in Figure 5. In Figure 5a, we consider the molal compositions of cations A^+, B^{2+} and anions X^-, Y^{2-} ($[Z^{3-}]$ is ignored). The two coordinates therefore are

$$R(A^+) = \frac{[A^+]}{[A^+]+2[B^{2+}]}, \quad \text{and} \tag{19a}$$

$$R(X^-) = \frac{[X^-]}{[X^-]+2[Y^{2-}]}. \tag{19b}$$

In effect, Figure 5a is the projection of the phase diagram of Figure 4 onto the $S1S2S4S5$ face of the prism as viewed through the $S3-S6$ edge. As $[Z^{3-}]$ is ignored, the saturation varieties in which the only anion present is Z^{3-} ($S3$ saturation, $S6$ saturation, and $S3S6$ double saturation) cannot be plotted on this projection. However, the information on these saturation varieties is not lost as they can be plotted on the

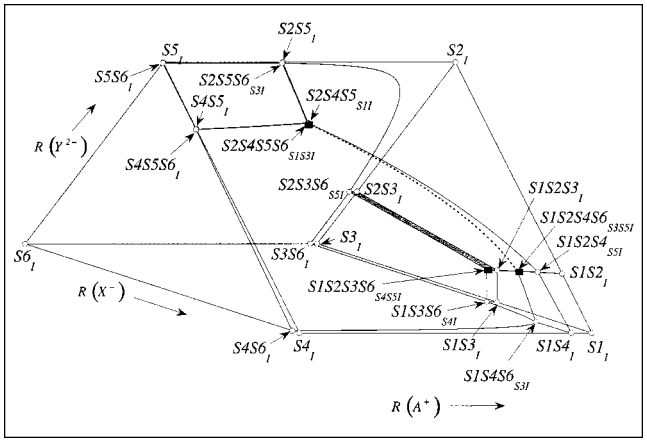

Figure 4. Solvent-less projection (prism diagram) for Example 2.

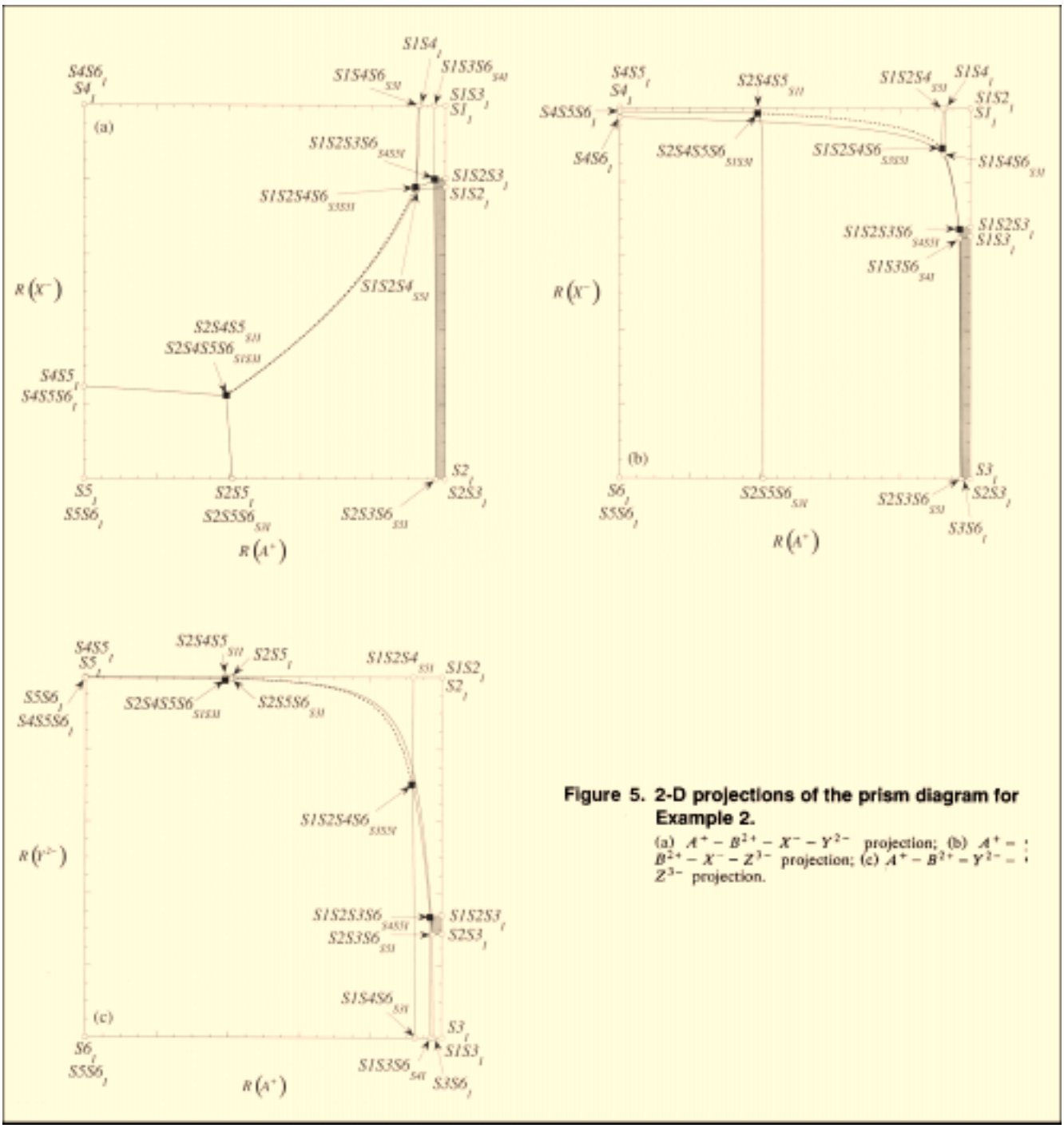

Figure 5. 2-D projections of the prism diagram for Example 2.

(a) $A^+ - B^{2+} - X^- - Y^{2-}$ projection; (b) $A^+ - B^{2+} - X^- - Z^{3-}$ projection; (c) $A^+ - B^{2+} - Y^{2-} - Z^{3-}$ projection.

remaining two projections. The projections of Figures 5b and 5c do not consider $[Y^{2-}]$ and $[X^-]$, respectively, The coordinates used are

$$\text{for Figure 5b:}\quad R(A^+) = \frac{[A^+]}{[A^+]+2[B^{2+}]},$$

$$R(X^-) = \frac{[X^-]}{[X^-]+3[Z^{3-}]}, \qquad (20a)$$

$$\text{for Figure 5c:}\quad R(A^+) = \frac{[A^+]}{[A^+]+2[B^{2+}]},$$

$$R(Y^{2-}) = \frac{2[Y^{2-}]}{2[Y^{2-}]+3[Z^{3-}]}. \qquad (20b)$$

As before, the saturation varieties are identified from the saturation variety matrix (not shown for the sake of brevity). For example, the $S2S3$ double saturation variety is a surface

Table 8. Ionic Products for Example 3

Index	Chemical Formula	Salt Name	Ionic Product
$S1$	$NaCl$	Halite	$(\gamma^*_{Na^+}[Na^+])(\gamma^*_{Cl^-}[Cl^-])$
$S2$	Na_2SO_4	Thenardite	$(\gamma^*_{Na^+}[Na^+])(\gamma^*_{SO_4^{2-}}[SO_4^{2-}])^{1/2}$
$S3$	$Na_2SO_4 \cdot 10\,H_2O$	Mirabilite	$(\gamma^*_{Na^+}[Na^+])(\gamma^*_{SO_4^{2-}}[SO_4^{2-}])^{1/2}(\gamma_W x_W)^5$
$S4$	KCl	Sylvite	$(\gamma^*_{K^+}[K^+])(\gamma^*_{Cl^-}[Cl^-])$
$S5$	K_2SO_4	Arcanite	$(\gamma^*_{K^+}[K^+])(\gamma^*_{SO_4^{2-}}[SO_4^{2-}])^{1/2}$
$S6$	$NaK_3(SO_4)_2$	Glaserite	$(\gamma^*_{Na^+}[Na^+])^{1/4}(\gamma^*_{K^+}[K^+])^{3/4}(\gamma^*_{SO_4^{2-}}[SO_4^{2-}])^{1/2}$

bounded by edges connecting $S2S3_I$, $S1S2S3_I$, $S1S2S3S6_{S4S5I}$, and $S2S3S6_{S5I}$. This surface is shown as the shaded region on Figures 4 and 5. The $S2S4S6$ triple saturation variety is the edge connecting vertices $S1S2S4S6_{S3S5I}$ and $S2S4S5S6_{S1S3I}$. This edge is shown as a bold dashed curve on Figures 4 and 5.

Example 3: system with compound formation

As an example of the compound forming system, let us consider the reciprocal salt system $(Na^+, K^+)(Cl^-, SO_4^{2-})-H_2O$. We want to consider the solid-liquid phase behavior in the temperature range [273.15 K, 373.15 K]; the melting and boiling points of water. The four ions form four simple salts halite ($S1$), thenardite ($S2$), sylvite ($S4$), and arcanite ($S5$). Within the temperature range, the system also forms two compounds: a hydrate mirabilite ($S3$), and a double salt glaserite ($S6$). The chemical formulae and the ionic products of these salts are as listed in Table 8. The asymmetric molal activity coefficients for the ions and the symmetric activity coefficient for water are obtained using a simplified version of the extended UNIQUAC-Debye-Hückel model. The model, its parameters, and the details of the discussion on how these parameters are obtained is given by Nicolaisen et al. (1993) and is not repeated here. Let us begin by constructing the digraph for the isothermal isobaric phase behavior at 373.15 K and 1 atm.

The algorithm of Table 2 is used to screen the vertices from all possible choices. The results are shown in Table 9.

Table 9. Vertices and their Locations at 373.15 K (Example 3)

Vertex	Location $R(Na^+)$	Location $R(Cl^-)$	Location $1/s$
One Saturated Salt			
$S1_W$	1	1	0.152
$S2_{S3W}$	1	0	0.168
$S4_W$	0	1	0.134
$S5_W$	0	0	0.372
Two Saturated Salts			
$S1S2_{S3W}$	1	0.881	0.140
$S1S4_W$	0.517	1	0.105
$S2S6_{S3S5W}$	0.766	0	0.132
$S4S5_W$	0	0.955	0.130
$S5S6_{S2S3W}$	0.368	0	0.230
Three Saturated Salts			
$S1S2S6_{S3S4S5W}$	0.607	0.869	0.104
$S1S4S6_{S2S3S5W}$	0.529	0.915	0.099
$S4S5S6_{S1S2S3W}$	0.236	0.925	0.118

The maximum number of salts that can be saturated together is $m+n-1=2+2-1=3$. At this temperature and pressure, we have 3 vertices with three saturated salts, 5 vertices with two saturated salts, and 4 vertices with one saturated salt.

The adjacency matrix for the system is shown in Figure 6. The edges are identified by reading across the rows of the adjacency matrix. For example, vertex $S2S6_{S3S5W}$ is connected to vertex $S1S2S6_{S3S4S5W}$; salts $S2$ and $S6$ being saturated on this edge. The edges are calculated using the algorithm of Table 3.

The three independent coordinates for graphical representation are

$$R(Na^+) = \frac{[Na^+]}{[Na^+]+[K^+]}, \tag{21a}$$

$$R(Cl^-) = \frac{[Cl^-]}{[Cl^-]+2[SO_4^{2-}]}, \quad \text{and} \tag{21b}$$

$$\frac{1}{s} = \frac{1}{[Na^+]+[K^+]}. \tag{21c}$$

The solvent-less projection of the phase diagram is always 2-D. Figure 7 shows the solvent-less projection at 373.15 K. The figure also shows the saturation variety matrix at this temperature. The saturation varieties can be identified on the phase diagram by reading across the rows of this matrix. For example, edge $S4S5_W - S4S5S6_{S1S2S3W}$ represents the $S4S5$ double saturation variety and the $S6$ saturation variety is represented by the edges connecting vertices $S2S6_{S3S5W}$, $S5S6_{S2S3W}$, $S4S5S6_{S1S2S3W}$, $S1S4S6_{S2S3S5W}$, and $S1S2S6_{S3S4S5W}$. There are two interesting consequences of compound formation that can be noted from this phase diagram. First, salt $S3$ ($Na_2SO_4 \cdot 10H_2O$) is always unsaturated at this temperature. Second, the composition corresponding to salt $S6$ ($NaK_3(SO_4)_2$) (shown as the filled square on Figure 7) does not lie within its saturation variety. Such salts are said to be incongruently saturated.

Evolution of Saturation Varieties. It is interesting to see how compound formation influences the appearance and disappearance of saturation varieties with increasing temperature $\in$[273.15 K, 373.15 K] (Figure 8). Let us begin with the phase diagram at 273.15 K (Figure 8a). At this temperature, salt $S2$ is always unsaturated and the $S6$ saturation variety lies completely within the composition space (region shaded with dots). As the temperature increases, the locations of the

Adjacency Matrix

	$S1_W$	$S2_{S3W}$	$S4_W$	$S5_W$	$S1S2_{S3W}$	$S1S4_W$	$S2S6_{S3S5W}$	$S4S5_W$	$S5S6_{S2S3W}$	$S1S2S6_{S3S4S5W}$	$S1S4S6_{S2S3S5W}$	$S4S5S6_{S1S2S3W}$
$S1_W$	0	0	0	0	1	1	0	0	0	0	0	0
$S2_{S3W}$	0	0	0	0	1	0	1	0	0	0	0	0
$S4_W$	0	0	0	0	0	1	0	1	0	0	0	0
$S5_W$	0	0	0	0	0	0	0	1	1	0	0	0
$S1S2_{S3W}$	0	0	0	0	0	0	0	0	0	1	0	0
$S1S4_W$	0	0	0	0	0	0	0	0	0	0	1	0
$S2S6_{S3S5W}$	0	0	0	0	0	0	0	0	1	1	0	0
$S4S5_W$	0	0	0	0	0	0	0	0	0	0	0	1
$S5S6_{S2S3W}$	0	0	0	0	0	0	1	0	0	0	0	1
$S1S2S6_{S3S4S5W}$	0	0	0	0	0	0	0	0	0	0	1	0
$S1S4S6_{S2S3S5W}$	0	0	0	0	0	0	0	0	0	1	0	1
$S4S5S6_{S1S2S3W}$	0	0	0	0	0	0	0	0	0	0	1	0

Figure 6. Adjacency matrix at 373.15 K for Example 3.

vertices change. Most notably, vertices $S1S3S4_{S2S5S6W}$ and $S3S4S6_{S1S2S5W}$ move towards each other. They annihilate each other at 276.99 K, giving birth to two new vertices with three saturated salts, viz., $S1S3S6_{S2S4S5W}$ and $S1S4S6_{S2S3S5W}$. As a result, for $T > 276.99$ K, the $S6$ saturation variety is bounded by four edges instead of three as shown in the phase diagram at 277.65 K (Figure 8b). As the temperature increases further, the $S3S5S6_{S1S2S4W}$ vertex moves towards the bottom. When it finally reaches the bottom at 279.09 K, two new vertices with two saturated salts are formed. These vertices are $S3S6_{S2S5W}$ and $S5S6_{S2S3W}$. As the temperature increases beyond 279.09 K, these newly formed vertices keep drifting apart, thus enlarging the $S6$ saturation variety as shown on the phase diagram at 283.15 K (Figure 8c). As the temperature increases further, two events occur simultaneously at 288.23 K. Vertex $S1S3S6_{S2S4S5W}$ splits into two vertices $S1S2S6_{S3S4S5W}$ and $S2S3S6_{S1S4S5W}$ and vertex $S1S3_{S2W}$ splits into $S1S2_{S3W}$ and $S2S3_{S1W}$. This is the temperature at which $S2$ saturation variety first appears. As the temperature increases, the newly formed vertices drift further apart. This enlarges the $S2$ saturation variety and diminishes the $S3$ saturation variety. On the phase diagram at 298.15 K (Figure 8d), the $S2$ saturation variety is shown as the region shaded with lines. At 303.05 K, vertices $S2S3S6_{S1S4S5W}$, $S3S6_{S2S5W}$, and $S2S3_{S1W}$ collapse into vertex $S3_{S2W}$ to form vertex $S2_{S3W}$. At this temperature, the $S3$ saturation variety disappears completely. For $T > 303.05$ K, salt $S3$ is always unsaturated as can be seen from the phase diagram at 323.15 K (Figure 8e). The structure of the phase diagram does not change any further as the temperature is increased to the upper bound of 373.15 K (Figure 8f) although the locations of the vertices and the edges change.

Application to Process Synthesis

The main advantage of this systematic method is the ease with which it allows the design engineer to visualize and study the phase behavior of high-dimensional ionic systems. In this section, we will discuss in detail the application of the framework to the synthesis of a crystallization-based process flowsheet.

Let us consider the system of Example 3. We have two feedstreams, stream L1 that is saturated with $S3$ ($Na_2SO_4 \cdot 10H_2O$) at 273.15 K and stream L7 that is saturated with $S4$ (KCl) at 298.15 K. The objective is to separate salts $S1$ (NaCl), $S2$ (Na_2SO_4), and $S5$ (K_2SO_4) as products using crystallization. A feasible flowsheet for this task is shown in Figure 9. This flowsheet is loosely based on the process suggested by Efraim et al. (1996). The feedstream L1 is fed to crystallizer C1. This crystallizer is operated at 373.15 K as an evaporative crystallizer and salt $S2$ is removed as the product. The mother liquor (L2) is then mixed with the recycle streams from crystallizers C3 (L8) and C4 (L6) to form the feed to crystallizer C2 (L4). C2 operates at 298.15 K as a cooling crystallizer and salt $S6$ is separated as the product. The mother liquor from this crystallizer (L5) forms the feed to crystallizer C4. This is again an evaporative crystallizer operating at 373.15 K with salt $S1$ being the solid product. The mother liquor (L6) is recycled. Salt $S6$ separated from C2 is fed to the third crystallizer with the second feed stream (L7) and excess solvent (E3). C3 is a cooling crystallizer. It operates at 298.15 K and separates salt $S5$. The mother liquor (L8) is recycled as mentioned before. The crystallizer operating temperatures and stream data are listed in Table 10. Note that this flowsheet is one of several feasible alternatives. It may not be the optimal, both in terms of flowsheet structure and operating conditions. Let us now turn our attention to how the phase diagrams are useful in constructing this flowsheet.

Figure 10 depicts the operation of the flowsheet. The operation of the evaporative crystallizers C1 and C4 is shown on the phase diagram of Figure 10a (373.15 K) and the operation of the cooling crystallizers is shown on the phase diagram of Figure 10b (298.15 K). Small filled circles and bold material balance lines are used to depict the movements on the phase diagram. At 273.15 K, feed stream L1 is saturated with salt $S3$. If we go back to the phase diagram of Figure 8a, this stream corresponds to the vertex $S3_{S2W}$. As we have seen

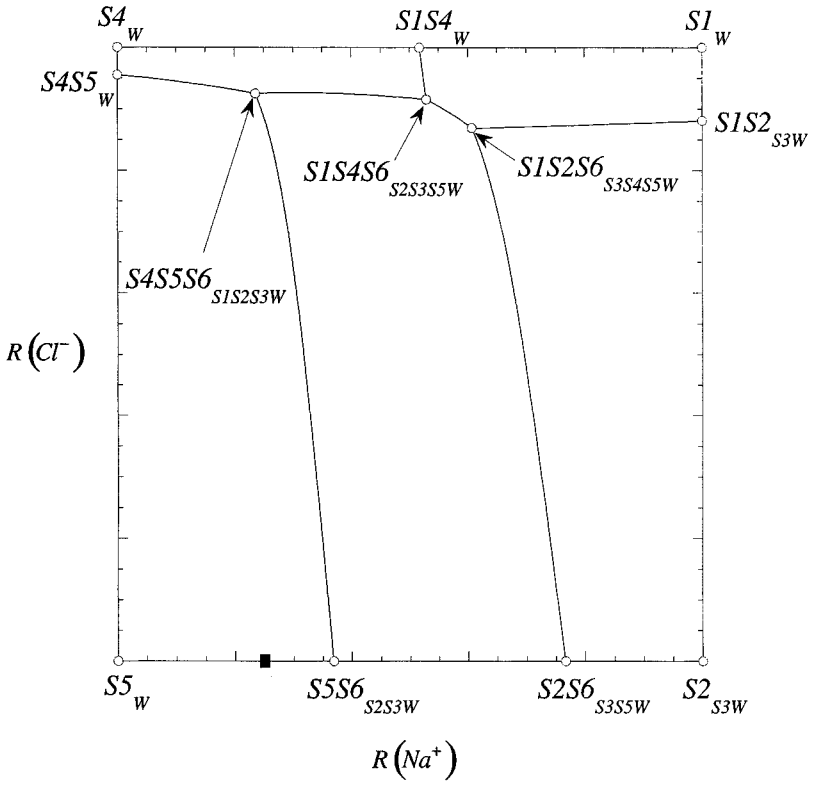

(a)

Saturation Variety Matrix

	$S1_W$	$S2_{S3W}$	$S4_W$	$S5_W$	$S1S2_{S3W}$	$S1S4_W$	$S2S6_{S3S5W}$	$S4S5_W$	$S5S6_{S2S3W}$	$S1S2S6_{S3S4S5W}$	$S1S4S6_{S2S3S5W}$	$S4S5S6_{S1S2S3W}$
$S1$–sat	1	0	0	0	1	1	0	0	0	1	1	0
$S2$–sat	0	1	0	0	1	0	1	0	0	1	0	0
$S4$–sat	0	0	1	0	0	1	0	1	0	0	1	1
$S5$–sat	0	0	0	1	0	0	0	1	1	0	0	1
$S6$–sat	0	0	0	0	0	0	1	0	1	1	1	1
$S1S2$–sat	0	0	0	0	1	0	0	0	0	1	0	0
$S1S4$–sat	0	0	0	0	0	1	0	0	0	0	1	0
$S1S6$–sat	0	0	0	0	0	0	0	0	0	1	1	0
$S2S6$–sat	0	0	0	0	0	0	1	0	0	1	0	0
$S4S5$–sat	0	0	0	0	0	0	0	1	0	0	0	1
$S4S6$–sat	0	0	0	0	0	0	0	0	0	0	1	1
$S5S6$–sat	0	0	0	0	0	0	0	0	1	0	0	1
$S1S2S6$–sat	0	0	0	0	0	0	0	0	0	1	0	0
$S1S4S6$–sat	0	0	0	0	0	0	0	0	0	0	1	0
$S4S5S6$–sat	0	0	0	0	0	0	0	0	0	0	0	1

(b)

Figure 7. Solvent-less projection and saturation variety matrix at 373.15 K for Example 3.

before, at 273.15 K salt $S2$ is always unsaturated. However, as the temperature is increased, the $S2$ saturation variety gradually appears and the $S3$ saturation variety gradually disappears. For $T > 303.05$ K, salt $S3$ is always unsaturated. Therefore, in crystallizer C1, we can separate $S2$ as a product (P1) from stream L1 by operating at $T > 303.05$ K and by removing sufficient amount of water. The operating temperature is chosen to be the boiling point of pure solvent at 1

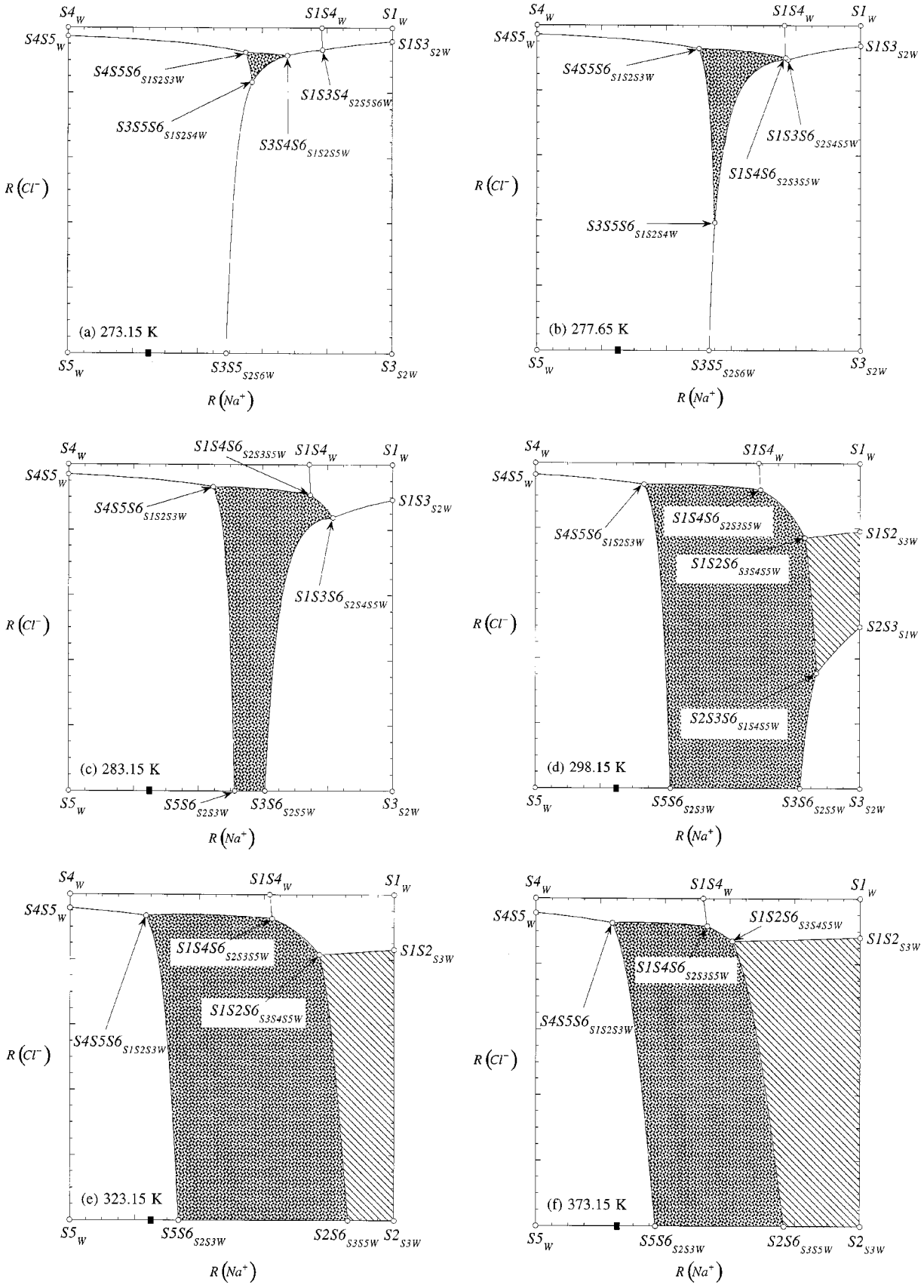

Figure 8. Evolution of saturation varieties for Example 3.

Solvent-less projections at (a) 273.15 K, (b) 277.65 K, (c) 283.15 K, (d) 298.15 K, (e) 323.15 K, (f) 373.15 K.

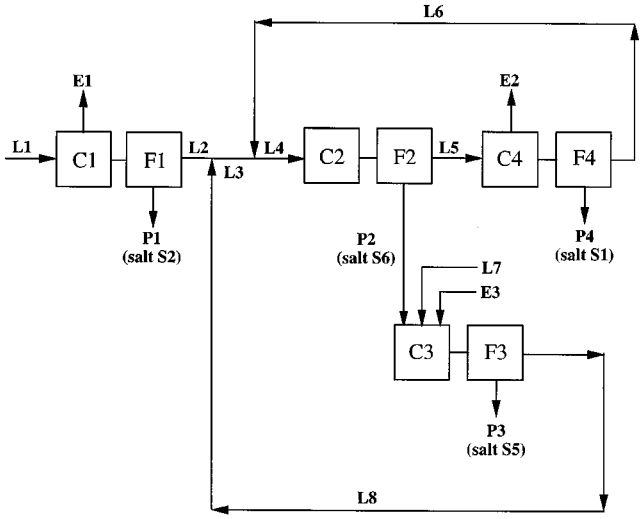

Figure 9. Flowsheet for separation of salts from the system of Example 3.

atm. Note that streams L1, L2, and P1 all lie at the same point on Figure 10a as the solvent coordinate is not plotted.

We have separated salt *S*2. The two other salts that remain to be separated are *S*1 and *S*5. The only other feedstream available is L7, which is saturated with salt *S*4 at 298.15 K (vertex $S4_W$). By mixing this feedstream with L2 at a suitable temperature, we can move into the *S*5 saturation variety and separate salt *S*5. However, then there is no way to cross over from the *S*5 saturation variety to the *S*1 saturation variety only by using temperature and solvent swings (we do not have any other process streams left). Therefore, we

Table 10. Crystallizer Temperatures and Stream Data for the Process of Figure 9

Crystallizer	Operating Temperature
C1 and C4	373.15 K
C2 and C3	273.15 K

Liquid Streams

Stream	$[Na^+]$	$[K^+]$	$[Cl^-]$	$[SO_4^{2-}]$	Solvent Molar Flow
L1*	0.657	0.0	0.0	0.3285	1.0
L2	6.068	0.0	0.0	3.034	0.051
L3	2.276	1.659	1.723	1.106	0.179
L4	4.962	3.103	6.839	0.613	0.776
L5	4.835	2.720	6.839	0.358	0.776
L6	5.769	3.536	8.374	0.465	0.597
L7**	0.0	4.671	4.671	0.0	0.066
L8	0.772	2.317	2.405	0.342	0.128

Vapor (Solvent) Streams

Stream	Molar Flow
E1	0.949
E2	0.179
E3	0.062

Solid (Salt) Streams

Stream	Molar Flow
P1 (Na_2SO_4)	0.0031
P2 ($NaK_3(SO_4)_2$)	0.0018
P3 (K_2SO_4)	0.0028
P4 (NaCl)	0.0056

*Solution saturated with $Na_2SO_4 \cdot 10\ H_2O$ at 273.15 K.
**Solution saturated with KCl at 298.15 K.
All flows are normalized with the solvent flow of stream L1.

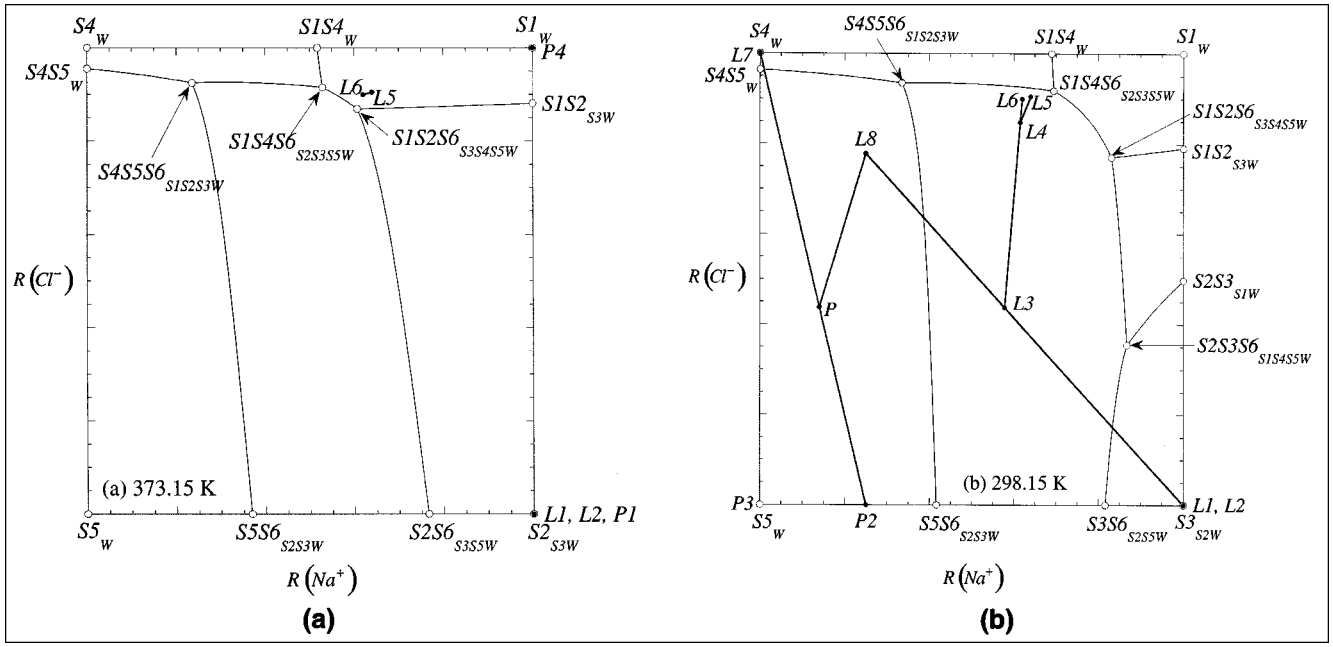

Figure 10. Operation of the flowsheet of Figure 9.

(a) Solvent-less projection depicting the operation of crystallizers C1 and C4 (373.15 K); (b) solvent-less projection depicting the operation of crystallizers C2 and C3 (298.15 K).

will not be able to separate $S1$. However, there is a way out. As we have noted earlier, salt $S6$ is incongruently saturated. Recall that the composition corresponding to $S6$ always lies within the $S5$ saturation variety. If we mix L7 with salt $S6$ we will be able to separate salt $S5$ at a suitable temperature. Therefore, we need to separate $S6$ from L2 and in doing so move the mother liquor composition closer to the $S1$ saturation variety. This is done in crystallizer C2. As shown in the phase diagram of Figure 10b, L2 is mixed with recycle streams L8 and L6 to form L3. The composition of L3 lies within the $S6$ saturation variety but is extremely close to the $S1$ saturation variety. $S6$ is crystallized at 298.15 K as the product (P2) and the mother liquor has the composition corresponding to point L5. In crystallizer C3, $S6$ is mixed with feedstream L7, and additional solvent (required to ensure co-precipitation does not occur). The resulting composition (corresponding to point P) lies within the $S5$ saturation variety. $S5$ is separated (P3) at 298.15 K and the mother liquor (L8) is recycled.

Now let us go back to Figure 8. If we observe the evolution of the $S1$ saturation variety, we can see that as temperature increases, this variety expands to the left. Therefore, stream L5 (which was within the $S6$ saturation variety but close to the $S1$ saturation variety at 298.15 K) could lie in the $S1$ saturation variety at higher temperatures. Indeed, this is the case as seen from Figure 10a. At 373.15 K, we can separate salt $S1$ as the product (P4) with appropriate amount of solvent being removed. The mother liquor L6 is recycled as discussed before. The operating temperature is chosen as 373.15 K as this is the boiling point of pure solvent at 1 atm pressure.

Conclusions

Visualization of high-dimensional phase diagrams of multicomponent ionic systems is crucial for process synthesis. Although much work has been done in the area of thermodynamic model development and experimental validation, the problem of representation of the phase behavior of solutions of strong electrolytes has not received enough attention. In this contribution, we have presented a systematic procedure for this task.

The geometry of the phase diagrams in high-dimensional composition space is captured in a digraph and its associated matrices. A systematic procedure allows the user to generate and plot these digraphs at any temperature and pressure using a set of independent coordinates. These coordinates are shown to be similar in principle to the other transformed coordinates in the literature. We have also suggested appropriate use of projections to plot the phase diagrams. This allows the user to study the phase behavior in its entirety, although it is impossible to plot the high-dimensional phase diagram on the plane of the paper.

The minimum information this framework requires is the salts that can be formed in the range of temperatures and pressures of interest, and their solubility products. This information can be easily obtained from various standard sources (Linke and Seidell, 1965; Silcock, 1979; Zemaitis et al., 1986). If data on ionic activities for a thermodynamically consistent model are for available, even more accurate phase diagrams can be generated for process synthesis.

Acknowledgment

We express our appreciation to the National Science Foundation, Grant No. CTS-9908667, for support of this research.

Notation

$A = (a_{ij})$ = adjacency matrix
$B = (b_{ij})$ = invariance matrix
c = number of components
E = set of edges of a digraph
e_{ij} = edge $\in E$ joining vertices v_i and v_j
f = degrees of freedom
F = molar flow rate
$\hat{F}$ = transformed molar flow rate
G = digraph
i, j, k, p, q = indices
K_i^I = ionic product for salt i
K_i^{sp} = solubility product for salt i
m = number of cations
$[M_i]$ = molality of ion M_i
M_I = molecular weight of solvent I
n = number of anions
P = pressure
r = number of independent chemical reactions
R = universal gas constant
$R(M_i), R(N_i)$ = independent coordinates related to ionic compositions
$1/s$ = independent coordinate related to solvent composition
$S = (s_{ij})$ = saturation variety matrix
T = temperature
v_i = vertex $\in V$
x_i = mole fraction of component i

Greek letters

γ_i = activity coefficient of component i
μ_i = chemical potential of component i
ν_i = stoichiometric coefficient of component i

Subscripts

e_{ij} = along edge e_{ij}
I = solvent
P = at constant pressure
T = at constant temperature
v_i = on vertex v_i
W = water

Superscripts

I = ionic system
sat = at saturation

Literature Cited

Ainsworth, S. J., "Soaps and Detergents," *Chem. Eng. News*, **34** (Jan. 24, 1994).

Berry, D. A., and K. M. Ng, "Separation of Quaternary Conjugate Salt Systems by Fractional Crystallization," *AIChE J.*, **42**, 2162 (1996).

Berry, D. A., and K. M. Ng, "Synthesis of Reactive Crystallization Processes," *AIChE J.*, **43**, 1737 (1997).

Biggs, N., *Algebraic Graph Theory*, 2nd ed., University Press, Cambridge (1993).

Cisternas, L. A., "Optimal Design of Crystallization-Based Separation Schemes," *AIChE J.*, **45**, 1477 (1999).

Efraim, I., S. Lampert, and C. Holdengraber, "Co-Production of Potassium Sulfate, Sodium Sulfate, and Sodium Chloride," U.S. Patent No. 5,552,126 (1996).

Fuyuhiro, A., K. Yamanari, and Y. Shimura, "Solubility Isotherms of Reciprocal Salt-Pairs of Optically Active Cobalt(III) Complexes," *Bull. Chem. Soc. Japan*, **52**(1), 90 (1979).

Jongema, P., "Process of the Precipitation of Sodium Chloride," U.S. Patent No. 5,221,528 (1993).
Linke, W. F., and A. Seidell, *Solubilities of Inorganic and Metal Organic Compounds*, American Chemical Society, Washington, DC (1965).
Liu, Y., and S. Watanasari, "Successfully Simulate Electrolyte Systems," *Chem. Eng. Prog.*, **95**(10), 25 (1999).
Mehta, V. C., "Process for Recovering Lithium from Salt Brines," U.S. Patent No. 4,723,962 (1988).
Meissner, H. P., and J. W. Tester, "Activity Coefficients of Strong Electrolytes in Aqueous Solutions," *Ind. Eng. Chem. Process Des. Develop.*, **11**, 128 (1972).
Meissner, H. P., and C. L. Kusik, "Aqueous Solutions of Two or More Strong Electrolytes: Vapor Pressures and Solubilities," *Ind. Eng. Chem. Process Des. Develop.*, **12**, 205 (1973).
Meissner, H. P., and C. L. Kusik, "Double Salt Solubilities," *Ind. Eng. Chem. Process Des. Develop.*, **18**, 391 (1979).
Meul, T., "Process for Resolution of Racemates of 2,2-Dimethyl Cyclopropane Carboxylic Acid," U.S. Patent No. 5,166,417 (1992).
Nicolaisen, H., P. Rasmussen, and J. M. Sørensen, "Correlation and Prediction of Mineral Solubilities in the Reciprocal Salt System $(Na^+, K^+)(Cl^-, SO_4^{2-}) - H_2O$ at 0–100°C," *Chem. Eng. Sci.*, **48**, 3149 (1993).
Paul, E. L., and C. B. Rosas, "Challenges for Chemical Engineers in the Pharmaceutical Industry," *Chem. Eng. Prog.*, **86**(12), 17 (1990).
Pérez Cisneros, E. S., R. Gani, and M. L. Michelsen, "Reactive Separation Systems: I. Computation of Physical and Chemical Equilibrium," *Chem. Eng. Sci.*, **52**, 527 (1997).
Pitzer, K. S., "Thermodynamics of Electrolytes: I. Theoretical Basis and General Equations," *J. Phys. Chem.*, **77**, 268 (1973).
Pitzer, K. S., "Thermodynamics of Electrolytes: V. Effects of Higher-Order Electrostatic Terms," *J. Sol. Chem.*, **4**, 249 (1975).
Pitzer, K. S., *Thermodynamics*, 3rd ed., McGraw Hill, New York (1995).
Pressly, T. G., and K. M. Ng, "Process Boundary Approach to Separations Synthesis," *AIChE J.*, **45**, 1939 (1999).
Rafal, M., R. Young, and J. Berthold, "Industrial Applications of Aspen OLI," *Aspen World 2000*, Orlando, FL (2000).
Samant, K. D., and K. M. Ng, "Synthesis of Extractive Reaction Processes," *AIChE J.*, **44**, 1323 (1998).
Samant, K. D., D. A. Berry, and K. M. Ng, "Representation of High-Dimensional, Molecular Solid-Liquid Phase Diagrams," *AIChE J.*, , **46**, 2435 (2000).
Sander, B., Aa. Fredenslund, and P. Rasmussen, "Calculation of Solid-Liquid Equilibria in Aqueous Solutions of Nitrate Salts Using an Extended UNIQUAC Equation," *Chem. Eng. Sci.*, **41**, 1197 (1986).
Schroer, J. W., C. Wibowo, and K. M. Ng, "Synthesis of Chiral Crystallization Processes," *AIChE J.*, **47**, 369 (2001).
Silcock, H. L., *Solubilities of Inorganic and Organic Compounds*, Pergamon, Oxford (1979).
Stinson, S. C., "Chiral Drugs," *Chem. Eng. News*, **38** (Sept. 19, 1994).
Ung, S., and M. F. Doherty, "Vapor-Liquid Phase Equilibrium in Systems with Multiple Chemical Reactions," *Chem. Eng. Sci.*, **50**, 23 (1995a).
Ung, S., and M. F. Doherty, "Synthesis of Reactive Distillation Systems with Multiple Equilibrium Chemical Reactions," *Ind. Eng. Chem. Res.*, **34**, 2555 (1995b).
Waller, K. V., and P. M. Mäkilä, "Chemical Reaction Invariants and Variants and Their Use in Reactor Modeling, Simulation, and Control," *Ind. Eng. Chem. Process Des. Dev.*, **20**, 1 (1981).
Wibowo, C., and K. M. Ng, "Unified Approach for Synthesizing Crystallization-Based Separation Processes," *AIChE J.*, **46**, 1400 (2000).
Zemaitis Jr., J. F., D. M. Clark, M. Rafal, and N. C. Scrivner, *Handbook of Aqueous Electrolyte Thermodynamics*, AIChE, New York (1986).

Appendix A: Rank of the Invariance Matrix

Let us consider a system with m cations (M_1, M_2, ..., M_m) with positive charges of magnitudes (z_{M_1}, z_{M_2}, ..., z_{M_m}), n anions (N_1, N_2, ..., N_n) with negative charges of magnitudes (z_{N_1}, z_{N_2}, ..., z_{N_n}), and one solvent I. There are mn simple salts, S_1, S_2, ..., S_{mn}. The invariance matrix for the system takes the following form

$$\begin{array}{c|ccccc} & S_1 & S_2 & \cdots & S_{mn} & I \\ \hline K_1 \equiv M_1 & b_{11} & b_{12} & \cdots & b_{1,mn} & 0 \\ \vdots & \vdots & \vdots & \cdots & \vdots & \vdots \\ K_m \equiv M_m & b_{m,1} & b_{m,2} & \cdots & b_{m,mn} & 0 \\ K_{m+1} \equiv N_1 & b_{m+1,1} & b_{m+1,2} & \cdots & b_{m+1,mn} & 0 \\ \vdots & \vdots & \vdots & \cdots & \vdots & \vdots \\ K_{m+n} \equiv N_n & b_{m+n,1} & b_{m+n,2} & \cdots & b_{m+n,mn} & 0 \\ I & 0 & 0 & \cdots & 0 & 1 \end{array} \tag{A1}$$

The ions are renamed as K_1 to K_{m+n} for the sake of convenience. b_{ij} represents the stoichiometric coefficient of ion K_i in salt S_j.

Let us first ignore the row (and the column) corresponding to solvent I. The remaining part of matrix B can be written as

$$\tilde{B} = \begin{bmatrix} b_{11} & b_{12} & \cdots & b_{1,mn} \\ b_{21} & b_{22} & \cdots & b_{2,mn} \\ \vdots & \vdots & \ddots & \vdots \\ b_{m+n,1} & b_{m+n,2} & \cdots & b_{m+n,mn} \end{bmatrix} = \begin{bmatrix} b_1^T \\ b_2^T \\ \vdots \\ b_{m+n}^T \end{bmatrix} \tag{A2}$$

With this definition, we can write

$$M_C = \tilde{B} N_C \tag{A3}$$

$M_C \in \Re^{(m+n)\times 1}$ is a column vector of molal compositions of the ions ($M_{C_i} = [K_i]$) and $N_C \in \Re^{mn\times 1}$ is a column vector of number of moles of salts per kg of solvent I. We can also write the above equation as

$$M_{C_i} = [K_i] = b_i^T N_C \tag{A4}$$

The condition of electroneutrality states that

$$\sum_{i=1}^{m} z_{K_i}[K_i] = \sum_{i=m+1}^{m+n} z_{K_i}[K_i] \tag{A5}$$

We can rewrite this equation as

$$\sum_{i=1}^{m+n-1} \alpha_i [K_i] = \alpha_{m+n}[K_{m+n}] \tag{A6}$$

where

$$\alpha_i = \begin{cases} z_{K_i} & \text{for } i = 1, 2, \ldots, m, \\ -z_{K_i} & \text{for } i = m+1, m+2, \ldots, m+n-1, \\ z_{K_i} & \text{for } i = m+n. \end{cases} \tag{A7}$$

Substituting from Eq. A4, we get

$$\sum_{i=1}^{m+n-1} \alpha_i b_i^T N_C = \alpha_{m+n} b_{m+n}^T N_C$$

$$\Rightarrow \sum_{i=1}^{m+n-1} \alpha_i b_i^T = \alpha_{m+n} b_{m+n}^T \quad \text{(A8)}$$

This implies that the last row of matrix $\tilde{B}$ can be expressed as a linear combination of the first $m+n-1$ rows. Therefore $m+n-1$ of the $m+n$ rows of $\tilde{B}$ are linearly independent [rank $(\tilde{B}) = m+n-1$].

Now let us consider the row (and the column) corresponding to the solvent I. Clearly, this row is linearly independent of the others as the solvent does not contain any ions or salts. Therefore, accounting for this row, a total of $m+n$ rows of the invariance matrix B are linearly independent. Therefore, rank $(B) = m+n$.

Appendix B: Linearity of Material Balance Equations

Let us consider the system of m cations, n anions, and a solvent. We have two liquid streams with molar flow rates $F1$ and $F2$ and compositions x^{F1} and x^{F2}, respectively. When mixed, they form a stream with molar flow rate $F3$ and composition x^{F3}. The material balance equations can be written as

$$F1x^{F1} + F2x^{F2} = F3x^{F3} \quad \text{(B1)}$$

For ions, the molalities are related to the mole fractions as (for example for cation M_k)

$$[M_k] = \frac{x_{M_k}}{x_I M_I} \quad \text{(B2)}$$

Using these relations, the material balance equations can be written in terms of molalities as

$$F1x_I^{F1}[M_i]^{F1} + F2x_I^{F2}[M_i]^{F2} = F3x_I^{F3}[M_i]^{F3} \quad i = 1, 2, \ldots, m,$$

$$F1x_I^{F1}[N_i]^{F1} + F2x_I^{F2}[N_i]^{F2} = F3x_I^{F3}[N_i]^{F3} \quad i = 1, 2, \ldots, n,$$

$$F1 + F2 = F3. \quad \text{(B3)}$$

To plot the phase diagrams, we use $m+n-1$ independent coordinates as discussed in the text. Let us write the material balance equations in terms of these independent coordinates. We will do this for one of the independent coordinates $R(M_i)$. The analysis can be easily extended for the remaining coordinates. For streams $F1$, $F2$, and $F3$, we can write

$$R^{F1}(M_i) = \frac{z_{M_i}[M_i]^{F1}}{\sum_{j=1}^{m} z_{M_j}[M_j]^{F1}}, \quad R^{F2}(M_i) = \frac{z_{M_i}[M_i]^{F2}}{\sum_{j=1}^{m} z_{M_j}[M_j]^{F2}},$$

$$R^{F3}(M_i) = \frac{z_{M_i}[M_i]^{F3}}{\sum_{j=1}^{m} z_{M_j}[M_j]^{F3}} \quad \text{(B4)}$$

Using the material balance equations, we can write $R^{F3}(M_i)$ as

$$R^{F3}(M_i) = \frac{z_{M_i}[M_i]^{F3}}{\sum_{j=1}^{m} z_{M_j}[M_j]^{F3}} = \frac{z_{M_i}F3x_I^{F3}[M_i]^{F3}}{\sum_{j=1}^{m} z_{M_j}F3x_I^{F3}[M_j]^{F3}}$$

$$= \frac{z_{M_i}F1x_I^{F1}[M_i]^{F1} + z_{M_i}F2x_I^{F2}[M_i]^{F2}}{\sum_{j=1}^{m} z_{M_j}F3x_I^{F3}[M_j]^{F3}} \quad \text{(B5)}$$

Upon further rearrangement we get

$$\left(F3x_I^{F3}\sum_{j=1}^{m} z_{M_j}[M_j]^{F3}\right)R^{F3}(M_i)$$

$$= \left(F1x_I^{F1}\sum_{j=1}^{m} z_{M_j}[M_j]^{F1}\right)\frac{z_{M_i}[M_i]^{F1}}{\sum_{j=1}^{m} z_{M_j}[M_j]^{F1}}$$

$$+ \left(F2x_I^{F2}\sum_{j=1}^{m} z_{M_j}[M_j]^{F2}\right)\frac{z_{M_i}[M_i]^{F2}}{\sum_{j=1}^{m} z_{M_j}[M_j]^{F2}}$$

$$\text{or} \quad \hat{F}3R^{F3}(M_i) = \hat{F}1R^{F1}(M_i) + \hat{F}2R^{F2}(M_i). \quad \text{(B6)}$$

$\hat{F}1$, $\hat{F}2$, and $\hat{F}3$ as defined above are the transformed molar flow rates. Similar analysis for the other independent coordinates also yields the same transformed flow rates. In general, the molar flow rates are transformed as

$$\hat{F} = Fx_I^F \sum_{j=1}^{m} z_{M_j}[M_j]^F \quad \text{(B7)}$$

Clearly, the transformation preserves the linearity of the material balance equations and the lever rule is still valid. However, the weights for the lever rule are transformed.

Appendix C: Compatibility of Salt Pairs

Consider a simple ionic system with cations M_1^+, M_2^+, anions N_1^-, N_2^-, and solvent I. The ions can form four salts M_1N_1 ($S1$), M_1N_2 ($S2$), M_2N_1 ($S3$), and M_2N_2 ($S4$). Note that we have considered all ions to be monovalent for the simplicity of representation. The following arguments are equally valid for simple ionic systems with multivalent ions.

There are two salt pairs ($S1$, $S4$) and ($S2$, $S3$) that do not have a common ion. At the specified temperature and pressure, one of these two salt pairs is compatible. Let us assume that the pair ($S1$, $S4$) is compatible. The system will thus have two vertices with three saturated salts, viz., $\upsilon_1 \equiv S1S2S4_{S3I}$ and $\upsilon_2 \equiv S1S3S4_{S2I}$. From the SLE condition, at vertex υ_1

$$K_{S1}^I = K_{S1}^{sp}, \qquad K_{S2}^I = K_{S2}^{sp},$$

$$K_{S3}^I < K_{S3}^{sp}, \qquad K_{S4}^I = K_{S4}^{sp}. \quad \text{(C1)}$$

and at vertex υ_2

$$K_{S1}^I = K_{S1}^{sp}, \qquad K_{S2}^I < K_{S2}^{sp},$$

$$K_{S3}^I = K_{S3}^{sp}, \qquad K_{S4}^I = K_{S4}^{sp}. \quad \text{(C2)}$$

Note that at any composition

$$K^I_{S1}K^I_{S4} = K^I_{S2}K^I_{S3} \tag{C3}$$

Using the above three equations, we get

$$K^{sp}_{S1}K^{sp}_{S4} < K^{sp}_{S2}K^{sp}_{S3} \tag{C4}$$

Therefore, the compatible salt pair is the one for which the product of the solubility products is lesser.

Appendix D: Note on Complex Ionic Systems

In the main body of this article, we have focused our attention on solutions of strong electrolytes. In general, ionic systems can exhibit more complex behavior that may be categorized as:

(1) Weak electrolytic systems
(2) Systems with complex intermediate ions
(3) Systems with dissociable solvent

Our framework for representation of phase behavior is not limited to strong electrolytic systems. It is universally applicable to systems with complex behavior as discussed in the following subsections.

Solutions of weak electrolytes

In solutions of weak electrolytes, the salts do not dissociate completely. The solid phase consists of the salts and the liquid phase consists of the solvent, the constitutive ions, and the undissociated salts in molecular form. Let us reconsider the system with m cations (M_1, M_2, …, M_m) with positive charges of magnitudes (z_{M_1}, z_{M_2}, …, z_{M_m}), n anions (N_1, N_2, …, N_n) with negative charges of magnitudes (z_{N_1}, z_{N_2}, …, z_{N_n}), and one solvent I. Let us consider a salt $S = \upsilon_M M_i \upsilon_N N_j$ that does not dissociate completely in solution. The criterion for SLE is still the same (the chemical potential of the salt in solid phase be equal to the sum of the chemical potentials of its constituents). Therefore, for salt S, at saturation

$$K^I_S = K^{sp}_S(T) \tag{D1}$$

The liquid phase also contains the salt in molecular form. Obviously, the chemical potential of molecular S in liquid phase is the same as the chemical potential of the constituent ions in the liquid phase. We can write the chemical potential of the molecular S in liquid phase as

$$\mu_{S,\text{liq}} = \mu^*_{S,\text{liq}} + RT \ln\left(\gamma^*_{S,\text{liq}}[S]\right) \tag{D2}$$

Here again, asterisk superscript indicates that infinite dilution standard state is used and the activity coefficients are based on molalities. By equating the chemical potentials, we can write

$$\frac{K^I_S}{\gamma^*_{S,\text{liq}}[S]} = \exp\left[-\frac{1}{RT}\left(\frac{\mu^*_{M_i}}{\upsilon_N} + \frac{\mu^*_{N_j}}{\upsilon_M} - \frac{\mu^*_{S,\text{liq}}}{\upsilon_M\upsilon_N}\right)\right] = K^d_S \tag{D3}$$

K^d_S is the dissociation constant for salt S.

Incomplete dissociation of salts does not affect the invariance matrix and its rank. It simply gives rise to additional species (molecular salts in liquid phase) and additional equations of the above form corresponding to each of these species. Therefore, the number and form of the independent coordinates, the adjacency rules, generation of adjacency and saturation variety matrices, and the compatibility test for salt pairs all remain the same. The only change occurs in the algorithms for calculation of the vertices and the edges of the digraph.

For example, let us consider the algorithm of Table 1. We are considering a vertex $\in V^I_{PT}$, at which the system has p cations (M_1, M_2, …, M_p), q anions (N_1, N_2, …, N_q), and the solvent. ($[M_{p+1}] = \cdots = [M_m] = [N_{q+1}] = \cdots = [N_n] = 0$). At this vertex, we have a total of pq weakly dissociating salts of which $p + q - 1$ are saturated. Therefore, we now have a total of $p + q + pq$ variables ($[M_i]$, $i = 1, 2, \ldots, p$, $[N_i]$, $i = 1, 2, \ldots, q$, and $[S_i]$, $i = 1, 2, \ldots, pq$) that we have to calculate by solving the following $p + q + pq$ equations:

- $p + q - 1$ phase equilibrium equations for the saturated salts

$$K^{sp}_i = K^I_i, \qquad i = 1, 2, \ldots, p + q - 1,$$

- pq dissociation equations for all salts

$$K^d_{S_i} = \frac{K^I_{S_i}}{\gamma^*_{S_i,\text{liq}}[S_i]}, \qquad i = 1, 2, \ldots, pq, \text{ and}$$

- One equation for electroneutrality of the system

$$\Sigma^p_{i=1} z_{M_i}[M_i] = \Sigma^q_{i=1} z_{N_i}[N_i].$$

Systems with complex intermediate ions

Let us consider the above system again. Let us assume that the system forms complex ions from its constituent ions, for example, $L = aM_ibN_j$ (here $a/b \neq z_{N_j}/z_{M_i}$). Only neutral species can precipitate from the solution. Therefore, the SLE equations stay the same. In addition, we have equations that arise from equating the chemical potentials of the complex intermediate ions to the corresponding sum of the chemical potentials of their constituent ions. For example for the ion L, we have

$$\frac{\mu_L}{ab} = \frac{\mu_{M_i}}{b} + \frac{\mu_{N_j}}{a} \tag{D4}$$

This gives rise to

$$\left(\gamma^*_{M_i}[M_i]\right)^{1/b}\left(\gamma^*_{N_j}[N_j]\right)^{1/a} = \exp\left[-\frac{1}{RT}\left(\frac{\mu^*_{M_i}}{b} + \frac{\mu^*_{N_j}}{a} - \frac{\mu^*_L}{ab}\right)\right] = K^d_L \tag{D5}$$

K^d_L is the dissociation constant for the intermediate ion L.

Each complex intermediate ion corresponds to an additional species which has an additional equation of the above form associated with it. Therefore, these ions do not affect

the invariance matrix and its rank, the number and form of the independent coordinates, the adjacency rules, generation of adjacency and saturation variety matrices, and the compatibility test for salt pairs. As before, the only change occurs in the algorithms for calculation of the vertices and the edges of the digraph. In these algorithms, we now have to include the complex intermediate ions and their dissociation equations.

Systems with dissociable solvent

In systems with dissociable solvent, we do not have to consider the row and column elements of the invariance matrix that correspond to the solvent. As the solvent dissociates, these elements will be replaced by its constituent ions. If we have a system with m cations, n anions, and one dissociable solvent, we have a total of $m+n+2$ ions. The rank of the invariance matrix is then $m+n+1$ and we need a total of $m+n$ independent coordinates to represent the phase behavior. The system has $m+1$ cations and $n+1$ anions. Therefore, we can choose m coordinates related to the cations and n coordinates related to the anions. The solvent coordinate is no longer needed as it is accounted for in the above $m+n$ coordinates.

In the above discussion we have considered these complexities independently. However, they can be present simultaneously in a system. These combinations can also be clearly handled easily as shown. The framework for automatic generation of phase diagrams is valid for all systems.

Manuscript received Mar. 22, 2000, and revision received July 27, 2000.